

1 Lactobacilli and other gastrointestinal microbiota of *Peromyscus leucopus*, reservoir host for  
2 agents of Lyme disease and other zoonoses in North America

3 Short title: Gastrointestinal microbiota of *Peromyscus leucopus*

4

5 Ana Milovic <sup>1</sup>, Khalil Bassam <sup>1,2</sup>, Hanjuan Shao <sup>1</sup>, Ioulia Chatzistamou <sup>3</sup>, Danielle M. Tufts <sup>4</sup>,  
6 Maria Diuk-Wasser <sup>4</sup>, and Alan G. Barbour <sup>1,5\*</sup>

7

8 <sup>1</sup> Department of Microbiology & Molecular Genetics, University of California Irvine, Irvine,  
9 California, United States of America

10 <sup>2</sup> Faculty of Medicine, American University of Beirut, Beirut, Lebanon

11 <sup>3</sup> Department of Pathology, Microbiology and Immunology, School of Medicine, University of  
12 South Carolina, Columbia, South Carolina, United States of America

13 <sup>4</sup> Department of Ecology, Evolution and Environmental Biology, Columbia University, New  
14 York, New York, United States of America

15 <sup>5</sup> Department of Medicine, University of California Irvine, Irvine, California, United States of  
16 America

17 \* Corresponding author

18 Email: [abarbour@uci.edu](mailto:abarbour@uci.edu)

## 19 Abstract

20 The cricetine rodent *Peromyscus leucopus* is an important reservoir for several human  
21 zoonoses, including Lyme disease, in North America. Akin to hamsters, the white-footed  
22 deermouse has been unevenly characterized in comparison to the murid *Mus musculus*. To  
23 further understanding of *P. leucopus*' total genomic content, we investigated gut microbiomes of  
24 an outbred colony of *P. leucopus*, inbred *M. musculus*, and a natural population of *P. leucopus*.  
25 Metagenome and whole genome sequencing were combined with microbiology and microscopy  
26 approaches. A focus was the genus *Lactobacillus*, four diverse species of which were isolated  
27 from forestomach and feces of colony *P. leucopus*. Three of the species--*L. animalis*, *L. reuteri*, and  
28 provisionally-named species "L. peromysci"--were identified in fecal metagenomes of wild *P.*  
29 *leucopus* but not discernibly in samples from *M. musculus*. *L. johnsonii*, the fourth species, was  
30 common in *M. musculus* but absent or sparse in wild *P. leucopus*. Also identified in both colony  
31 and natural populations were a *Helicobacter* sp. in feces but not stomach, and a *Tritrichomonas* sp.  
32 protozoan in cecum or feces. The gut metagenomes of colony *P. leucopus* were similar to those of  
33 colony *M. musculus* at the family or higher level and for major subsystems. But there were  
34 multiple differences between species and sexes within each species in their gut metagenomes at  
35 orthologous gene level. These findings provide a foundation for hypothesis-testing of functions  
36 of individual microbial species and for interventions, such as bait vaccines based on an  
37 autochthonous bacterium and targeting *P. leucopus* for transmission-blocking.

38

## 39 Introduction

40 Epigraph: “I have always looked at problems from an ecological point of view, by  
41 placing most emphasis not on the living things themselves, but rather on their inter-  
42 relationships and on their interplay with surroundings and events.” René Dubos, 1981 (1, 2)

43

44 *Peromyscus leucopus*, the white-footed deermouse, is one of the most abundant wild  
45 mammals in central and eastern United States and adjacent regions of Canada and Mexico (3, 4).  
46 The rodent is an omnivore, consuming a variety of seeds, such as oak acorns, as well as insects  
47 and other invertebrates. Its wide geographic range extends from rural areas to suburbs and  
48 even cities, and it is especially common in areas where humans and wildland areas interface (5).  
49 Conditions permitting, *P. leucopus* is procreatively proliferant, with 20 or more litters during a  
50 female’s period of fecundity (6).

51 Although commonly called a “mouse”, this species and other members of the genus  
52 *Peromyscus* belong to the family Cricetidae, which includes hamsters and voles, and not the  
53 family Muridae, which includes *Mus* and *Rattus*. The pairwise divergence time for the genera  
54 *Peromyscus* and *Mus* is estimated to be ~27 million years ago (7, 8), approximately the time since  
55 divergence of the family Hominidae, the great apes and hominids, from Cercopithecidae, the  
56 Old World monkeys (7, 9). While only a minority of a birth cohort of *P. leucopus* typically  
57 survive the predation and winter conditions of their first year in nature (10, 11), in captivity

58 *Peromyscus* species can live twice as long as the laboratory mouse or rat (12). *P. leucopus* differs  
59 in its social behavior and reproductive physiology from rodents that are traditional  
60 experimental models (13, 14).

61 *P. leucopus* also merits special attention as a natural host and keystone reservoir for  
62 several tickborne zoonoses of humans (reviewed in (15)). These include Lyme disease,  
63 babesiosis, anaplasmosis, a form of relapsing fever, ehrlichiosis, and a viral encephalitis. For  
64 humans these infections are commonly disabling and sometimes fatal, but *P. leucopus* is  
65 remarkably resilient in the face of persistent infections with these pathogens, singly or in  
66 combination. How this species tolerates infections to otherwise thrive as well as it does is poorly  
67 understood.

68 *P. leucopus'* importance as a pathogen reservoir, its resilience in the face of infection, and  
69 its appealing features as an animal model (6, 16), prompted our genetic characterization of this  
70 species, beginning with sequencing and annotating its nuclear and mitochondrial genomes (17,  
71 18). The present study represents the third leg of this project, namely the microbial portion of  
72 the total animal "genome" for this species. Given the development of bait-delivered oral  
73 vaccines targeting *P. leucopus* (19) and plans to genetically modify and release this species (20,  
74 21), pushing ahead on these interventional fronts without better understanding *Peromyscus*  
75 microbiota, the gastrointestinal (GI) tract's in particular, seemed shortsighted.

76 Accordingly, we carried out a combined microbiologic and metagenomic study of the GI  
77 microbiome of *P. leucopus*. Our study focused on animals of a stock colony that has for many

78 years been the major source of animals for different laboratories and spin-off breeding  
79 programs, including our own, in North America. The study extended to samples of *P. leucopus*  
80 deermice in their natural environments and, for a comparative animal, vivarium-reared *Mus*  
81 *musculus* under similar husbandry. While our investigations revealed similarities between the  
82 microbiota of the white-footed deermouse and the house mouse, there were also notable  
83 differences. These included a greater abundance and diversity of lactobacilli in *P. leucopus*. The  
84 investigation of four *Lactobacillus* species, particularly in their niches in the stomach of *P.*  
85 *leucopus*, was a special emphasis. A comparison of the GI microbiota of a natural population of  
86 *P. leucopus* and the stock colony animals revealed several species in common, albeit with larger  
87 variance among the wild animals .

88

## 89 **Results and discussion**

### 90 **High coverage sequencing of fecal metagenome**

91 Since there was only limited information in the literature on the GI microbiota of *P.*  
92 *leucopus* (22, 23), we began with untargeted assessment of microbiome constituents and their  
93 diversity in a sample of fecal pellets collected from two adult males and two adult females of  
94 the same birth cohort and shipment.

95 DNA was extracted and used for library construction; 332,279,332 paired-end reads of  
96 average length 247 nt were obtained after quality control and trimming of adapters. The mean

97 % GC content was 47; 90% of the trimmed reads had PHRED scores of  $\geq 30$ . The reads were  
98 characterized as to families of bacteria, parasites, and DNA viruses at the metagenomic server  
99 MG-RAST (<http://mgrast.org>). Annotated proteins accounted for 65% of the reads, followed by  
100 unknown proteins at 34%, and then ribosomal RNA (rRNA) genes at 0.8%. The rarefaction  
101 curve became asymptotic at 200,000 reads and a species count of 9000 (Fig S1 of Supplementary  
102 information). The alpha diversity was 250 species. By phylum 94% of the matched reads were  
103 either Bacteroidetes (60%) or Firmicutes (34%) (Fig S2 of Supplementary information). Higher  
104 level functional categories included carbohydrates (16.4% of reads), clustering-based  
105 subsystems (14.8%), protein metabolism (8.9%), amino acids and derivatives (7.8%), RNA  
106 metabolism (6.6%), and DNA metabolism (5.7%) (Fig S3 of Supplementary information).

107 A portion of the DNA was also submitted for commercial 16S rRNA metagenomics  
108 analysis of microbiota. As illustrated in Fig 1 and detailed in Tables S1 and S2 of Supplementary  
109 information, for the 20 most abundant taxa at the family or higher, there was concordance  
110 between the methods in the rankings. The most common families by the metagenomic  
111 accounting were members of the gram-negative bacterial order Bacteroidales (*Bacteroidaceae*,  
112 *Porphyromonadaceae*, *Prevotellaceae*, and *Rikenellaceae*), the gram-positive phylum Actinobacteria  
113 (*Bifidobacteriaceae* and *Coriobacteriaceae*), or the gram-positive phylum Firmicutes (*Bacillaceae*,  
114 *Enterococcaceae*, *Lactobacillaceae*, unclassified Clostridiales, *Eubacteriaceae*, *Lachnospiraceae*,  
115 *Peptococcaceae*, *Ruminococcoceae*, Thermoanaerobacterales Family III, *Erysipelotrichaceae*, and

116 *Veillonellaceae*). Two exceptions were organisms of the families *Spirochaetaceae* of the phylum  
117 Spirochaetes and *Helicobacteraceae* of the phylum Proteobacteria.

118 **Fig 1.** Scatter plot of relative abundances of commonly occurring bacterial families or orders in  
119 fecal metagenomes of *Peromyscus leucopus* LL stock by 16S ribosomal RNA gene criteria (*x*-axis)  
120 and by genome-wide gene (*y*-axis). The values of the two methods were normalized by *Z*-score.  
121 The different taxa are indicated in the graph capital letters, which defined in the box to right.  
122 The linear regression curve and its 95% confidence interval is shown. The coefficient of  
123 determination ( $R^2$ ) value and the Kruskal-Wallis (K-W) test by ranks *p* value are given.

124 A de novo assembly yielded 16,945 ungapped contigs of  $\geq 10$  kb from 197,369,943 reads  
125 and totaling 385 Mb of sequence with an average coverage of 104X. Of the total, 219 contigs  
126 were  $\geq 100$  kb in length and with  $\geq 30$ X coverage. These were used in searches of non-redundant  
127 nucleotide and protein databases for provisional classifications. The identified taxa included  
128 Bacteroidales, Clostridia, *Clostridiaceae*, Erysipelotrichales, *Lactobacillaceae*, *Muribaculaceae*,  
129 Firmicutes, and *Spirochaetaceae*. Three organisms represented among the high coverage contigs  
130 could be unambiguously classified as to species: *Lactobacillus animalis*, which is considered in  
131 detail below, and two *Parabacteroides* species: *distasonis* and *johnsonii*. Another *Lactobacillus*  
132 species represented among the highly ranked contigs could not be identified with a known  
133 species represented in the database (24).

134 Among the high coverage contigs were also representatives of Rhodospirillales of the  
135 class Alphaproteobacteria, *Mycoplasmataceae* of Mollicutes, and the little-characterized group of

136 bacteria called Elusimicrobia (25). Nearly as prevalent were organisms closely related to the  
137 phylum-level designation *Candidatus* Melainabacteria (26). On the list of organisms identified by  
138 searches with metagenomic contigs of databases and cumulatively accounting for 95% of the  
139 matched reads were the unexpected finding of the protozoan taxon *Trichomonadidae* with 41,614  
140 or 0.12% of the reads (Table S2 of Supplementary information). *Enterobacteriaceae* at 0.3%  
141 accounted for a relatively small proportion of matched reads.

142         As in humans (27), *Bacteroidaceae*, *Lachnospiraceae*, *Prevotellaceae*, and *Ruminococcaceae*  
143 were abundant in the gut metagenome and cumulatively accounted for approximately half of  
144 the identified families in the *P. leucopus* sample. One difference between humans and this *P.*  
145 *leucopus* sample was the much higher prevalence in *P. leucopus* of the family *Lactobacillaceae*,  
146 which on average represented only ~0.2% of the metagenome in a European population (27) and  
147 by 16S sequencing  $\leq 0.4\%$  on the fecal microbiota in other studies (28). A higher proportion of  
148 lactobacilli in the fecal microbiota was previously noted in other rodents (29).

## 149 **Selected taxa**

### 150 *Escherichia coli*

151         Although *Enterobacteriaceae* were infrequently represented among the metagenomic  
152 sequences, their cultivability under routine laboratory conditions and the availability of a vast  
153 database prompted our isolation of *Enterobacteriaceae* from LL stock *P. leucopus* fecal pellets on  
154 selective media. The predominant isolate on the plates was an *Escherichia coli*, which we



155 designated LL2. The whole genome sequence of isolate LL2's chromosome and plasmids was  
 156 sequenced and assembled using a hybrid of long reads and short reads (Table 1) for an overall  
 157 coverage of 90X. The chromosome in two contigs of 3.4 Mb and 1.6 Mb totaled 5.0 Mb with a GC  
 158 content of 50%.

159

Table 1. Resources from this study					
Organism and strain	Description	BioProject	BioSample	SRA or MG-RAST <sup>a</sup>	Accession No.
<i>Lactobacillus johnsonii</i> LL8	2,045,501 bp WGS chromosome; 40 contigs	<a href="#">PRJNA58909</a> <u>1</u>	<a href="#">SAMN1326652</a> <u>1</u>	<a href="#">SRX7128459</a>	<a href="#">WKKC00000000</a>
<i>Lactobacillus johnsonii</i> LL8	75,746 bp plasmid	<a href="#">PRJNA58909</a> <u>1</u>	<a href="#">SAMN1326652</a> <u>1</u>	<a href="#">SRX7128459</a>	<a href="#">CM019125</a>
<i>Escherichia coli</i> LL2	Chromosome; 3,345,873 and 1,610,537 bp contigs	<a href="#">PRJNA53383</a> <u>8</u>	<a href="#">SAMN1146894</a> <u>4</u>	<a href="#">SRR9087223</a> <a href="#">SRR9087224</a>	<a href="#">VBVB01000001</a> <a href="#">VBVB01000002</a>
<i>Escherichia coli</i> LL2	121,192 bp plasmid	<a href="#">PRJNA53383</a> <u>8</u>	<a href="#">SAMN1146894</a> <u>4</u>	<a href="#">SRR9087223</a> <a href="#">SRR9087224</a>	<a href="#">CM017030</a>
<i>Escherichia coli</i> LL2	90,617 bp plasmid	<a href="#">PRJNA53383</a> <u>8</u>	<a href="#">SAMN1146894</a> <u>4</u>	<a href="#">SRR9087223</a> <a href="#">SRR9087224</a>	<a href="#">CM017032</a>
<i>Escherichia coli</i> LL2	56,474 bp plasmid	<a href="#">PRJNA53383</a> <u>8</u>	<a href="#">SAMN1146894</a> <u>4</u>	<a href="#">SRR9087223</a> <a href="#">SRR9087224</a>	<a href="#">CM017031</a>

Gut metagenome	50-450 kb contigs of fecal metagenome	<a href="#">PRJNA54031</a> <u>7</u>	<a href="#">SAMN1153372</a> <u>0</u>	<a href="#">mgm4799371</a> <u>3</u> <a href="#">mgm4799372</a> <u>3</u>	<a href="#">JAAGKN00000000</a> <u>0</u>
Uncultured <i>Helicobacter</i> sp. LL4	290,716 bp 172,100 bp 203,294 bp chromosome fragments	<a href="#">PRJNA54031</a> <u>7</u>	<a href="#">SAMN1153372</a> <u>0</u>	<a href="#">mgm4799371</a> <u>3</u> <a href="#">mgm4799372</a> <u>3</u>	<a href="#">MN577567</a> <a href="#">MN577568</a> <a href="#">MN577569</a>
Uncultured <i>Helicobacter</i> sp. LL4	16S ribosomal RNA gene, partial	n.a. <sup>b</sup>	n.a.	n.a.	<a href="#">MT114577</a>
Uncultured Candidatus Melainabacteria bacterium isolate LL20	270,170 bp chromosome fragment	<a href="#">PRJNA54031</a> <u>7</u>	<a href="#">SAMN1153372</a> <u>0</u>	<a href="#">mgm4799371</a> <u>3</u> <a href="#">mgm4799372</a> <u>3</u>	<a href="#">MN577570</a>
Uncultured Elusimicrobia bacterium LL30	232,820 bp 215,518 bp chromosome fragments	<a href="#">PRJNA54031</a> <u>7</u>	<a href="#">SAMN1153372</a> <u>0</u>	<a href="#">mgm4799371</a> <u>3</u> <a href="#">mgm4799372</a> <u>3</u>	<a href="#">MN577571</a> <a href="#">MN577572</a>
Uncultured Clostridiales bacterium LL40	438,773 bp chromosome fragment	<a href="#">PRJNA54031</a> <u>7</u>	<a href="#">SAMN1153372</a> <u>0</u>	<a href="#">mgm4799371</a> <u>3</u> <a href="#">mgm4799372</a> <u>3</u>	<a href="#">MN577573</a>
Uncultured <i>Spirochaetaceae</i> bacterium LL50	277,828 bp chromosome fragment	<a href="#">PRJNA54031</a> <u>7</u>	<a href="#">SAMN1153372</a> <u>0</u>	<a href="#">mgm4799371</a> <u>3</u>	<a href="#">MN577574</a>

				<a href="#">mgm4799372.</a>	
				<u>3</u>	
Uncultured <i>Prevotella</i> sp. LL70	456,702 bp 379,405 bp chromosome fragments	<a href="#">PRJNA54031</a> <u>7</u>	<a href="#">SAMN1153372</a> <u>0</u>	<a href="#">mgm4799371.</a> <u>3</u> <a href="#">mgm4799372.</a> <u>3</u>	<a href="#">MN990733</a> MN990734
Uncultured Rhodospirillales bacterium LL75	145,048 bp 150,471 bp 130,339 bp 104,625 bp 177,737 bp chromosome fragments	<a href="#">PRJNA54031</a> <u>7</u>	<a href="#">SAMN1153372</a> <u>0</u>	<a href="#">mgm4799371.</a> <u>3</u> <a href="#">mgm4799372.</a> <u>3</u>	<a href="#">MN990728</a> MN990729 <a href="#">MN990730</a> <a href="#">MN990731</a> <a href="#">MN990732</a>
Uncultured <i>Mycoplasmatacea</i> e bacterium LL85	126,601 bp 100,243 bp chromosome fragments	<a href="#">PRJNA54031</a> <u>7</u>	<a href="#">SAMN1153372</a> <u>0</u>	<a href="#">mgm4799371.</a> <u>3</u> <a href="#">mgm4799372.</a> <u>3</u>	<a href="#">MN991199</a> MN991200
Uncultured Muribaculaceae bacterium LL71	125,326 bp 103,384 bp chromosome fragments	<a href="#">PRJNA54031</a> <u>7</u>	<a href="#">SAMN1153372</a> <u>0</u>	<a href="#">mgm4799371.</a> <u>3</u> <a href="#">mgm4799372.</a> <u>3</u>	<a href="#">MT002444</a> MT002445
<i>Tritrichomonas</i> sp. LL5	1,501 bp of small subunit ribosomal RNA	<a href="#">PRJNA54031</a> <u>7</u>	<a href="#">SAMN1392068</a> <u>3</u>	<a href="#">mgm4864879.</a> <u>3</u>	<a href="#">MN120899</a>
<i>Tritrichomonas</i> sp. LL5	989 bp partial iron hydrogenase gene of	<a href="#">PRJNA54031</a> <u>7</u>	<a href="#">SAMN1392068</a> <u>3</u>	<a href="#">mgm4864879.</a> <u>3</u>	<a href="#">MN985504</a>

	hydrogenosom e				
<i>Tritrichomonas</i> sp. LL5	5298 bp fragment with DNA polymerase type B, organellar and viral family protein	<a href="#">PRJNA54031</a> <u>7</u>	<a href="#">SAMN1392068</a> <u>3</u>	<a href="#">mgm4864879.</a> <u>3</u>	<a href="#">MT002461</a>
Uncultured <i>Lactobacillus</i> sp. ("peromysci") BI7442	<i>rpsA</i> , <i>ftsK</i> , <i>ftsZ</i> , <i>dnaA</i> , <i>dnaN</i> , <i>recD</i> , <i>ileS</i> , <i>recA</i> , <i>topA</i>	<a href="#">PRJNA59361</a> <u>8</u>	<a href="#">SAMN1348286</a> <u>2</u>	<a href="#">SRX7285441</a>	<a href="#">MN792760</a> - <a href="#">MN792768</a>
Uncultured <i>Lactobacillus</i> <i>animalis</i> 7442BI	51 large and small ribosomal proteins	<a href="#">PRJNA59361</a> <u>8</u>	<a href="#">SAMN1348286</a> <u>2</u>	<a href="#">SRX7285441</a>	<a href="#">MN817867</a> - <a href="#">MN817918</a>

160 <sup>a</sup> SRA, Sequence Read Archive accession number; MG-RAST, [mg-rast.org](http://mg-rast.org) metagenomics analysis server

161 sequence file number

162 <sup>b</sup> n.a., not applicable

163 *E. coli* LL2 had the following MLST schema types (<http://pubmlst.org> or

164 <http://enterobase.org>): Achtman ST-278, Pasteur ST-357, and ribosomal protein ST-122394. The

165 ribosomal protein profile was unique among thousands of isolates in the database. The 121 kb,

166 56.5 kb, and 91 kb plasmids of strain LL2 were similar to the following *E. coli* plasmids,

167 respectively: a 185 kb plasmid (NC\_007675) found in an avian strain, a 58 kb plasmid

168 (CP024858) of a multiply antibiotic-resistant human isolate, and an 89 kb plasmid (CM007643)  
169 in an organism isolated from sewage. *E. coli* LL2 was susceptible to ampicillin, ciprofloxacin,  
170 gentamicin, and sulfamethoxazole-trimethoprim by in vitro testing.

171 The chromosome was notable for the following: CRISPR-Cas1 and –Cas3 arrays; ISas1,  
172 ISNCY, IS3, IS110 and IS200 family transposases; restriction-modification systems; fimbria and  
173 curli biosynthesis and transport systems; type II toxin-antitoxin systems; and type II, type III  
174 and type VI secretion systems. The plasmids encoded fimbrial and pilin proteins, type I, type II,  
175 and type IV secretion systems, colicins, CdiA-type contact-dependent inhibition toxin, and three  
176 conjugative transfer systems, but no discernible coding sequences for antibiotic resistance.

177 Serial dilutions of feces of LL stock 20 animals (11 females and 9 males) in phosphate-  
178 buffered saline and plated on agar selective for gram-negative enteric bacteria yielded a mean  
179 (asymmetric 95% confidence interval) of 3,491 (677-18,010) colony-forming units (cfu) of *E. coli*  
180 per g of feces. This low density was consistent with the findings from metagenomic sequencing.

181 While the origin of this *E. coli* strain in the colony animals is obscure, it appears to be  
182 stably maintained among the gut microbiota of this population of *P. leucopus*. This adaptation  
183 may make it a candidate as a vector for delivering oral vaccines to this species (30).

## 184 *Lactobacillus*

185 We isolated lactobacilli from fecal pellets of stock colony *P. leucopus* on plates of selective  
186 medium that were incubated under microaerophilic and hypercapnic conditions at 37 °C. Four

187 different species were identified. The genomes of three of organisms, namely *L. animalis* strain  
188 LL1, *L. reuteri* strain LL7, and a new species, designated as *Lactobacillus* sp. LL6 and  
189 provisionally named as “*L. peromysci*”, have been reported (24). The fourth genome, of the LL8  
190 strain of *L. johnsonii*, is described first here (Table 1). *L. johnsonii*'s chromosome from cumulative  
191 contigs was 2,045,501 bp, about the same size as that of “*L. peromysci*” at 2,067,236 bp, but  
192 shorter than the 2,280,577 bp length for *L. animalis* and 2,205,740 bp for *L. reuteri*. The % GC  
193 content of “*L. peromysci*” at 33.5 was closer to *L. johnsonii* (34.4) than to either *L. animalis* (41.0)  
194 or *L. reuteri* (38.9).

195 Fig 2 is a distance phylogram of 1385 aligned sites of 16S ribosomal RNA genes for the  
196 four different lactobacilli. These were distributed across four major groups of the genus  
197 *Lactobacillus*. The phylogenetic relationships were examined in more depth by multilocus  
198 sequence typing of the 53 genes for ribosomal proteins. These were identified in the genomes,  
199 compared with other deposited sequences in the ribosomal MLST database  
200 (<https://pubmlst.org>) (31), concatenated, and then aligned with analogously concatenated DNA  
201 sequences from related species (Table S3 of Supplementary information). Bacteria with identical  
202 sequences for the 53 ribosomal protein genes were not found in the rMLST database of 133,460  
203 profiles. The % GC contents of the concatenated coding sequences were 39.5, 40.8, 42.2, and 42.3  
204 for *L. johnsonii*, “*L. peromysci*”, *L. reuteri*, and *L. animalis*, respectively. Fig 3 shows the distance  
205 phylograms for ~20 kb of aligned positions for the four species, each grouped with other strains  
206 or species within their respective phylogenetic clusters.

207 **Fig 2.** Neighbor-joining distance phylogram of 1420 aligned positions of 16S ribosomal RNA  
208 genes of the culture isolates of four *Lactobacillus* species from *Peromyscus leucopus* and selected  
209 other *Lactobacillus* spp. The sources for the accession numbers for the strains are given in  
210 Methods (*L. animalis*, *L. reuteri*, and “*L. peromysci*”) or in Table 1. The other organisms  
211 represented are from Reference RNA sequences database of the National Center for  
212 Biotechnology Information; the accession numbers are given after the species name. The scale  
213 for distance by criterion of observed differences is indicated. Percent bootstrap (100 iterations)  
214 support values of  $\geq 90\%$  at a node are shown.

215 **Fig 3.** Neighbor-joining distance phylograms of codon-aligned, concatenated nucleotide  
216 sequences for complete sets of ribosomal proteins of “*L. peromysci*” (panel A), *L. reuteri* (panel  
217 B), *L. animalis* (panel C), and *L. johnsonii* (panel D) of *P. leucopus* compared with *Lactobacillus* spp.  
218 (strain identifier) of other sources. The scales for distance by Jukes-Cantor criterion are  
219 indicated in each panel. Percent bootstrap (100 iterations) support values of  $\geq 75\%$  at a node are  
220 shown. In panels B and D the host animal or other origin for a given isolate are given in  
221 parentheses.

222 “*Lactobacillus peromysci*” was distant from other sequenced lactobacilli by rMLST  
223 (panel A), as well as by its 16S ribosomal RNA gene (Fig 2). The nearest taxon in the sequence  
224 alignment was *L. intestinalis*, which was first isolated from the intestines of *Mus musculus* and  
225 other murids (32). The unique ST for the rMLST for strain LL6 of this organism is 115326.

226 Draft and complete genomes of numerous *L. reuteri* strains have been sequenced, for  
227 example, strain Byun-re-01, which was isolated from *M. musculus* small intestine (33). Many of  
228 these are utilized in the fermented foods industry, such as production of kimchi, or as dietary  
229 supplements, but others were isolated as constituents of the GI microbiota of several varieties of  
230 animals. *L. reuteri* strain LL7 was in a cluster that mainly comprised isolates from *M. musculus*  
231 (panel B).

232 *L. animalis* and *L. murinus* are closely related species that primarily have been associated  
233 with GI microbiota of rodents and some other mammals. Isolate LL1 grouped with  
234 representatives of *L. animalis* in the analysis (panel C) and not *L. murinus* (34). LL1's 16  
235 ribosomal RNA sequence was identical to that of the type strain ATCC 35046 of *L. animalis* (35)  
236 at 1488 of 1489 positions (GCA\_000183825) (36). Another pair of closely-related species are *L.*  
237 *johnsonii* and *L. gasseri*, for which there are several sequenced genomes. The LL8 isolate from  
238 fecal pellets of *P. leucopus* clustered with *L. johnsonii* strains from mice and rats (panel D). More  
239 distant were strains of *L. johnsonii* isolated from humans and a bird; more distant still were  
240 representatives of *L. gasseri*.

241 Plasmids were identified in each of the four species on the basis of a circularly permuted  
242 sequence for a contig and presence of coding sequences that were homologous to known  
243 plasmid replication or partition proteins (Table 1). Large plasmids of 179 kb and 76 kb were  
244 present in *L. reuteri* and *L. johnsonii*, respectively. *L. animalis* and “*L. peromysci*” had small  
245 plasmids of 4 kb and 7 kb, respectively. Megaplasmids of greater than 100 kb have been



246 observed in other *Lactobacillus* spp. (37). In all genomes there was evidence of lysogenic  
247 bacteriophages or their remnants. All species except *L. reuteri* discernibly had coding sequences  
248 for Class I or Class III bacteriocins or their specific transport and immunity proteins (Table S4 of  
249 Supplementary information).

250 Table 2 summarizes differentiating genetic profiles among the four species for 11 selected  
251 genes or pathways. Two species, *L. reuteri* and “*L. peromysci*”, had coding sequences for a  
252 urease, which could provide for tolerance of acidic conditions, such as in the stomach. A urease  
253 had previously been identified in a *L. reuteri* strain that was considered a gut symbiont in  
254 rodents (38). The four species had *secY1-secA1* transport and secretion systems. Accessory Sec  
255 systems (*secY2-secA2*) were identified in genomes of *L. reuteri*, *L. johnsonii*, and *L. animalis* but  
256 not in “*L. peromysci*”. The LL7 strain of *L. reuteri* on its megaplasmid also had coding sequences  
257 for a third SecY-SecA system. An accessory Sec system was involved with adhesion and biofilm  
258 formation in the Lactobacillales bacterium *Streptococcus pneumoniae* (39). A coding sequence for  
259 an IgA protease was identified in *L. johnsonii* but not in the other three species. An IgA protease  
260 in another strain of *L. johnsonii* was associated with long-term persistence in the gut of mice (40).  
261 The presence or absence of other genes or pathways that differentiated between the four species  
262 were an L-rhamnose biosynthesis pathway in one species, a *luxS* gene associated with a quorum  
263 sensing system in *L. reuteri* and *L. johnsonii* (41), a type 1 CRISPR-Cas3 array in “*L. peromysci*”  
264 (42), pathways for thiamine biosynthesis (43) and for reduction of nitrate (44) in three species,

265 an arginine deiminase and its repressor in *L. reuteri* (45), and a type VII secretion system in *L.*  
 266 *animalis* (46).

Table 2. Selected genes and pathways in four species of *Lactobacillus* of the gastrointestinal microbiota of *Peromyscus leucopus*

Species	Urea se	<i>secY</i> 2- <i>secA</i> 2	<i>secY</i> 3- <i>secA</i> 3	IgA protease (pfam07 580)	L- rhamn ose pathwa y	<i>lux</i> S	Type 1 CRIS PR Cas	Thiamin e biosynth esis	Nitroreduc tase <i>nfnB-nifU</i>	Arginin e deimina se/ repress or	Type VII secreti on syste m
<i>reuteri</i>	+	+	+	-	-	+	-	-	-	+	-
<i>johnsonii</i>	-	+	-	+	-	+	-	+	+	-	-
<i>animalis</i>	-	+	-	-	-	-	-	+	+	-	+
“peromy sci”	+	-	-	-	+	-	+	+	+	-	-

267

268 Of the four species found in *P. leucopus* feces, only *L. johnsonii* and *L. reuteri* have been  
 269 commonly isolated from human feces (28). While various strains of *L. reuteri*, *L. johnsonii*, and  
 270 either *L. animalis* or the closely related *L. murinus* have been observed among the GI microbiota  
 271 of *M. musculus* representatives (47), an organism similar to “*L. peromysci*” has not. Whether  
 272 this is an indication of a restricted host range or a specific adaptation for this bacterium is  
 273 considered below.

274 ***Helicobacter***

275           Among the assembled metagenomic contigs were three totaling 666,100 bp of a  
276 *Helicobacter* genome (Table 1). The contigs had non-overlapping in genetic content, and blast  
277 searches with translated genes from each of the 3 contigs yielded the identical rankings of taxa  
278 for homologous proteins. On these bases, we concluded that the contigs represented a single  
279 type of *Helicobacter* bacterium, and designated it strain LL4. Using the DNA sequences for 53  
280 ribosomal proteins of this organism, we compared it with similar sets from other *Helicobacter*  
281 spp. (panel A of Fig 4; ). This analysis, as well as analysis of the 16S ribosomal RNA gene  
282 sequence from a fecal sample from another animal (Fig S5 of Supplementary information),  
283 showed that the organism was near-identical to orthologous sequences of *Helicobacter* sp. MIT  
284 05-5293 (accession JROZ02000000), which had been cultivated from a wild *P. leucopus* captured  
285 in Massachusetts (48; J.G. Fox, personal communication). This finding indicated that the  
286 organism was autochthonous for *Peromyscus* and had not been acquired from another rodent  
287 housed in the same vivarium. LL4 and MIT 05-5293 are in a cluster of species known as  
288 “enterohepatic” *Helicobacter* for their primary residence in the intestine rather than the stomach  
289 and for their frequent presence in liver tissue (49). These species may not be benign. *H. hepaticus*  
290 is associated with hepatitis, bowel inflammation, and carcinoma (50), and *H. typhlonius* is  
291 associated with reduced fecundity in mice (51).

292 **Fig 4.** Neighbor-joining distance phylograms of concatenated nucleotide (panel A) or amino  
293 sequences (panels B-C) of *Helicobacter* spp. (panel A), *Spirochaetaceae* bacteria (panel B),  
294 Mollicutes and Firmicutes bacteria (panel C) and Rhodospirillales bacteria (panel D) of gut

295 metagenome of *P. leucopus* and from other sources. The respective phylogenetic analyses used  
296 concatenated sequences of the following: ribosomal protein genes (panel A); the DNA gyrase A  
297 (GyrA), phenylalanyl t-RNA synthase, alpha subunit (PheS), and chromosomal replication  
298 initiator protein (DnaA) (panel B); DNA-directed RNA polymerase, beta-subunit (RpoB) (panel  
299 C); and DNA gyrase B (GyrB), tyrosyl t-RNA synthase (TyrS), and DnaA (panel D). The distance  
300 criteria were Jukes-Cantor for the codon-aligned nucleotide sequences and Poisson for amino  
301 acid sequences. The scales for distance are shown in each panel. Percent bootstrap (100  
302 iterations) support values of  $\geq 80\%$  at a node are shown.

### 303 *Spirochaetaceae*

304 Panels B, C, and D of Fig 4 are phylograms of three other types of bacteria that were  
305 identified among the high-coverage metagenomic contigs (Tables 1 and S5). The uncultured  
306 spirochete LL50 was placed in the genus *Treponema* by the MG-RAST analysis program. Yet  
307 species in this genus are highly divergent and include free-living organisms in a variety of  
308 environments, symbionts of termites, the agent of syphilis, and gut residents, such as *T.*  
309 *porcinum*, which was isolated from the feces of pigs (52). More distant still was the agent of  
310 Lyme disease, *Borrelia burgdorferi*, of the family *Borreliaceae* (53). In our view naming the  
311 organism as a “treponeme” would provide little insight about its role in the microbiome and  
312 may even be misleading.

### 313 **Seven other bacterial taxa**

314 The *Mycoplasmataceae* bacterium LL85 (panel C of Fig 4 and Table S5) was unlike any  
315 other mollicute represented in the database but was in cluster with vertebrate-associated  
316 species, like *M. pneumoniae*. But there is also deep branching in this tree, as the tree including as  
317 outgroup two Firmicutes shows. Panel D is a phylogram of selected alphaproteobacteria and  
318 includes the organism LL75 (Table S5). The algorithmic analysis identified this at the genus  
319 level as *Azospirillum*, which is a largely uncharacterized taxon with highly divergent members.  
320 While assignments as to genus or family are uncertain at this time, LL75 clustered within the  
321 order Rhodospirillales and not with rhizobacteria.

322 Table 1 lists five other types of novel bacteria that were identified in the *P. leucopus* gut  
323 metagenome and partially sequenced and annotated. These were a *Candidatus* Melainabacteria  
324 bacterium (isolate LL20), an Elusimicrobia bacteria (isolate LL30), a Clostridiales bacterium  
325 (isolate LL40), a *Prevotella* species (isolate LL70), and a *Muribaculaceae* bacterium (isolate LL71).  
326 *Candidatus* Melainabacteria is either a non-photosynthetic sister phylum of cyanobacteria or a  
327 class within the phylum Cyanobacteria (26). Besides a variety of environmental sources,  
328 including hot springs and microbial mats, these poorly-characterized organisms have also been  
329 identified in the feces of humans and other animals. The phylum Elusimicrobia, formerly  
330 “Termite Group 1” (54), is a strictly-anaerobic, deeply-branched lineage of gram-negative  
331 bacteria, representatives of which were first observed in the hindgut of termites (25). The family  
332 *Muribaculaceae* (formerly “family S24-7”) of the order Bacteroidales were first identified among

333 gut microbiota of mice and subsequently in the intestines of other animals, including humans  
334 and ruminants (55).

### 335 **DNA viruses**

336 Of 112,677,080 reads of the metagenome high-coverage sequencing of the LL stock  
337 animals, 97,147 (0.09%) were assigned to one of 28 DNA virus families. Three classifications  
338 accounted 92% of the reads: *Siphoviridae* (50%), which are bacteriophages with long contractile  
339 tails; *Myoviridae* (21%), which are bacteriophages with contractile tails; and “unclassified  
340 viruses” (21%). At the species level, 31,812 (68%) of the 46,904 *Siphoviridae*-matching reads  
341 mapped specifically to bacteriophages of *Lactobacillus* spp.

### 342 ***Tritrichomonas* protozoan**

343 Intestinal flagellated protozoa named “*Trichomonas muris*” or “*Tritrichomonas muris*”  
344 had previously been identified in wild *P. leucopus* and *P. maniculatus* (56). While laboratory mice  
345 are typically free of intestinal protozoa (57), the anaerobic *Tritrichomonas muris* has been  
346 reported in some populations of colony *M. musculus* (58). To further investigate the protozoa  
347 that were provisionally identified as “*Trichomondidae*” at the family level in the metagenome  
348 analysis, we euthanized 14 healthy adult animals (6 females and 8 males) and examined fresh  
349 cecal contents by phase microscopy. Six of the LL stock animals had been born at the PGSC  
350 facility, and 8 had been born at U.C. Irvine.

351 In each of the 14 animals examined there were numerous motile flagellates consistent in  
352 morphology with *T. muris* in their ceca (59). These were each at a cell density of  $\sim 10^6$  per  
353 milliliter of unconcentrated cecal fluid (Fig 5; S1 File). Entire ceca and their contents from two  
354 adult females and two adult males were subjected to DNA extraction, library preparation from  
355 the DNA, sequencing, and de novo assembly of contigs.

356 **Fig 5.** Photomicrograph of live *Tritrichomonas* flagellated protozoan in the cecal fluid of *P.*  
357 *leucopus* LL stock. Four organisms against the background of intestinal bacteria were visualized  
358 in the wet mount by differential interference microscopy. Bar, 10  $\mu\text{m}$ .

359 Fig 6 shows phylograms of nucleotide sequence of the small subunit (SSU) ribosomal  
360 RNA gene (panel A; Table S5) and of the partial amino acid sequence of the iron hydrogenase of  
361 the hydrogenosome of anaerobic protozoa (panel B; Table S5) (60). The SSU of isolate LL5  
362 indicates that it is probably synonymous with *Tritrichomonas muris*, for which only a SSU  
363 sequence was available. The sequence of the iron hydrogenase further supported placement in  
364 the genus *Tritrichomonas*. *Histomonas melagridis*, a sister taxon by this analysis, is recognized as a  
365 pathogen of poultry. Another sequence of the LL5 organism encodes a type B DNA polymerase  
366 (Table 1), which likewise matched closely with an ortholog in the *Tritrichomonas foetus* genome  
367 sequence (Fig S4 of Supplementary information). *T. foetus* is a sexually-transmitted pathogen of  
368 cattle (61) and a cause of chronic diarrhea in domestic cats (62).

369 **Fig 6.** Neighbor-joining distance phylograms of nucleotide (panel A) or amino acid (panel B)  
370 partial sequences of small subunit ribosomal RNA gene (rDNA) (panel A) and iron

371 hydrogenase protein (panel B) of *Tritrichomonas* sp. LL5 of *P. leucopus* and selected other  
372 parabasilids and other microbes. The distance criteria were observed differences for nucleotide  
373 alignment and Poisson for amino acid alignment. The scales for distance are shown in each  
374 panel. Percent bootstrap (100 iterations) support values of  $\geq 80\%$  at a node are shown.

375       Whether the *T. muris* is a commensal shared across natural populations of *Peromyscus* or  
376 a parasite acquired from another rodent during the colony's history in a vivarium remains to be  
377 determined. As related below, there is sequence evidence of the same or related organism in  
378 several wild animals. Whatever the case, these organisms may have an effect on immune  
379 responses of *P. leucopus*, as has been reported for *T. muris* in *M. musculus* (63-65), and their  
380 presence needs to be taken into account in interpreting experimental results in the laboratory  
381 and in applications for field interventions.

## 382 **Comparative study of GI microbiota of *P. leucopus* and *M. musculus***

383       The preceding study revealed several microbes that were either undescribed species or  
384 genera, e.g. “*L. peromysci*” or the *Candidatus* Melainabacteria bacterium, or new strains of  
385 known microbial species, e.g. *L. animalis* LL1 and *T. muris* LL4. These novelties notwithstanding,  
386 to what extent did the gut microbiota of this deermouse resemble that of the typical laboratory  
387 animal, a house mouse that was maintained under similar husbandry conditions, including  
388 diet? That question motivated the following experiment.



389 Fecal pellet samples from 20 adult *P. leucopus* (10 females and 10 males) and 20 adult  
390 BALB/c *M. musculus* (10 females and 10 males) were obtained and stored frozen at -80 °C until  
391 processing. All animals were approximately 10 weeks old. The animals were housed in the same  
392 vivarium facility, though in different rooms. The pellets were subjected to total DNA  
393 extractions, and paired-end Illumina sequencing with 250 cycles of indexed libraries were  
394 carried out. There were means (95% CI) of  $3.4 (3.1-3.7) \times 10^6$  post-quality control reads for *P.*  
395 *leucopus* samples and  $3.4 (3.2-3.6) \times 10^6$  for *M. musculus* samples (Tables S6 and S7 of  
396 Supplementary information).

397 The reproducibility between replicate library constructions from the same sample was  
398 assessed with quantitations of reads assigned by taxonomic family for specimens from seven *P.*  
399 *leucopus* among the 20 total. Pairwise coefficients of determination ( $R^2$ ) for the 91 possible  
400 combinations were calculated (Table S8 of Supplementary information). The mean (95% CI) of  
401  $R^2$  values were 0.999 (0.999-1.0) for the 7 pairs of replicates and 0.930 (0.915-0.944) for the 84  
402 non-replicate pairs. We concluded that most of the variation between samples was attributable  
403 to inter-specimen differences in the microbiota and not to technical issues in library preparation  
404 or sequencing.

405 The prevalences of different taxonomic families in the *P. leucopus* and *M. musculus* gut  
406 metagenomes were similar (left panel of Fig 7 and Table S9 of Supplementary information). But  
407 a few families stood out as either more or less common in the deermice. Notable among these  
408 were *Lactobacillaceae*, *Helicobacteriaceae*, and *Spirochaetaceae*, which were approximately 4x, 8x,

409 and 2x, respectively, more prevalent on average among microbiota of *P. leucopus* than in *M.*  
410 *musculus*. There was no evidence of *Tritrichomonas* sp. in the BALB/c mice by this analysis, but  
411 direct examination of intestinal contents was not carried out.

412 **Fig 7.** Scatter plots of log-transformed normalized reads of the gut metagenomes of 20 *P.*  
413 *leucopus* on the gut metagenomes of 20 *M. musculus* by bacterial families (left panel) or by  
414 function at the pathway level (right panel). The linear regression lines, their 95% confidence  
415 intervals, and coefficients of determination ( $R^2$ ) are shown. Selected families that are  
416 comparatively more or less prevalent in *P. leucopus* are indicated.

417 At the level of 86 operational KEGG pathways, the metagenomes of *P. leucopus* and *M.*  
418 *musculus* were nearly indistinguishable (right panel of Fig 7 and Table S10 of Supplementary  
419 information). But, as shown in the heat map of Fig 8, at the homologous gene level there were  
420 many differences between these two species and also between females and males within each  
421 species (Tables S12 and S13 of Supplementary information). Hierarchical clusters 2 and 4 of the  
422 analysis discriminated between mice and deermice regardless of sex, while clusters 1 and 3  
423 signified marked differences by sex and less so by species.

424 **Fig 8.** Heat map-formatted shading matrix of KEGG Orthology gene level annotations of gut  
425 metagenomes of *P. leucopus* and *M. musculus*. The annotations were generated by  
426 MicrobiomeAnalyst (<https://www.microbiomeanalyst.ca>). Columns are grouped by species and  
427 by sex within each species. Individual animal identifications are given on the  $x$ -axis below the  
428 heat map. Above the heat map are the log-transformed reads mapping to the genus

429 *Lactobacillus* for each animal's fecal sample. Clustering of rows of genes were by Pearson  
430 correlation coefficient. Four major clusters are labeled 1-4 on the *y*-axis. Scaling is by relative  
431 abundances from low (blue) to high (red).

432 As one example of differences between species, there was higher representation of genes  
433 of the mevalonate pathway in the gut metagenomes of *P. leucopus*. Beginning with acetyl-CoA  
434 and ending with isopentenyl pyrophosphate, the central intermediate in the biosynthesis of  
435 isoprenoids in all organisms (66), the coding sequences for the following ordered enzymes (with  
436 Enzyme Commission [EC] number) in the pathway were comparatively higher in frequency:  
437 acetyl-CoA C-acetyltransferase (EC:2.3.1.9), hydroxymethylglutaryl-CoA synthase (EC:2.3.3.10),  
438 hydroxymethylglutaryl-CoA reductase (EC:1.1.1.88), mevalonate kinase (EC:2.7.1.36),  
439 phosphomevalonate kinase (EC:2.7.4.2), and diphosphomevalonate decarboxylase (EC:4.1.1.33).

440 We further investigated specific differences between *P. leucopus* and *M. musculus* and  
441 between individual animals of each species in *Lactobacillus* spp. (67). This was achieved by  
442 mapping reads to references of the chromosome sequences of the four species that had been  
443 isolated from the feces of LL stock *P. leucopus*. The caveat is that the lactobacilli in the mice  
444 would not be expected to be identical to the deermouse strains used as references. Fig 9 shows  
445 box plots for *Peromyscus* on the left and for *Mus* on the right for data given in Table S11 of the  
446 Supplementary information. Included in the analysis of *P. leucopus* gut metagenome reads were  
447 selected other bacteria that had been frequently identified among the metagenomic contigs and  
448 then further characterized by partial genome sequencing (see above).

449 **Fig 9.** Box-whisker plots of log-transformed normalized reads of gut metagenomes of *P. leucopus*  
450 (left panel) and *M. musculus* (right panel) that mapped to chromosomes of *Lactobacillus* spp. or  
451 other bacteria by host species and grouped by sex. The references to which reads were mapped  
452 were complete chromosomes or partial chromosomes of organisms listed in Table 1.  
453 “*Lactobacillus*” in the first position of each panel were the cumulative reads for the four  
454 individual *Lactobacillus* species in this analysis.

455 All four species of the lactobacilli were represented in each of the 20 *P. leucopus*  
456 metagenomes. “*L. peromysci*” and *L. reuteri* tended to be the most common and consistently  
457 represented, while *L. johnsonii* and *L. animalis* varied more in prevalences between animals.  
458 Other bacteria were also identified in the samples of all or most of the individual animals. The  
459 *Spirochaetaceae* bacterium was ~10-fold less abundant than the cumulative *Lactobacillus* spp. in  
460 the *P. leucopus* samples.

461 The mean number of lactobacilli in aggregate were ~2-fold more prevalent in *P. leucopus*  
462 females than males of the species ( $t$ -test  $p = 0.03$ ). In *M. musculus* this sex difference for  
463 *Lactobacillus* was more pronounced; on average ~100-fold more reads from female mice mapped  
464 to *Lactobacillus* genomes than was found for male mice ( $t$ -test  $p < 0.001$ ). The differences in  
465 amounts of fecal lactobacilli in the sample plausibly account for cluster 3 of the heatmap of Fig  
466 8. *L. johnsonii* largely accounted for these differences between sexes in *M. musculus*; nearly all of  
467 the reads mapping to the *Lactobacillus* genus as a whole were mapping to the *L. johnsonii*  
468 genome. The three other species identified in *P. leucopus* were either not present or in much

469 lower numbers in this sampling of *M. musculus*. Strains of *L. johnsonii* have been commonly  
470 detected in feces of laboratory mice (68).

471 A limitation to the study was that the LL stock animals were outbred, and the BALB/c  
472 mice were inbred. An inbred lineage derived from the LL stock population was not available.  
473 On the other hand, this distinction provided a comparison of microbiome diversities between an  
474 outbred and inbred population. As expected, there was greater diversity among the outbred  
475 samples than the inbred (Fig 10). Another limitation was the dependence on fecal pellets  
476 collected at one time point. The samples were from similar age *P. leucopus* and *M. musculus* and  
477 were obtained from the animals and then processed on the same day, but for this study we did  
478 not assess variation within individuals over time.

479 **Fig 10.** Alpha diversity (left) and beta diversity (right) of gut metagenomes of outbred  
480 *Peromyscus leucopus* (green), a natural population of *P. leucopus* (blue), and inbred *Mus musculus*  
481 (red). Left panel, box-whisker plots of Shannon's Index for 20 BALB/c *M. musculus*, 20 LL stock  
482 colony *P. leucopus*, and 18 *P. leucopus* trapped on Block Island, RI. The 3 pairwise, 2-tailed *t*-test *p*  
483 values between the groups were  $\leq 0.02$ . Right panel, beta diversity by Bray-Curtis measure  
484 visualized by multi-dimensional scaling. The greater scattering of the samples from Block Island  
485 animals corresponded to the alpha diversity of this group.

486 **Lactobacilli of the stomach of *P. leucopus***

487 The differences between *P. leucopus* and *M. musculus* in the amount and species richness  
488 of the lactobacilli in their GI microbiota prompted further investigation of *P. leucopus* using  
489 histologic, microbiologic and genomic approaches. Fig 11 shows the gross morphology and  
490 histology of the stomach of representative LL stock *P. leucopus* animals (69). The difference  
491 between forestomach with its stratified squamous epithelium and the discrete region lined with  
492 glandular mucosa are indicated in the dissecting scope and higher magnification light  
493 microscope views.

494 **Fig 11.** Gross morphology and histology of the stomach of *Peromyscus leucopus* LL stock. The  
495 glandular mucosa portions of the stomach and the forestomach with stratified squamous  
496 epithelium are indicated. Panel A, whole stomach after dissection. Portions of the esophagus  
497 and small intestine are juxtaposed in the center in this view. Bar, 1 cm. Panel B, histology of  
498 hematoxylin and eosin-stained section of junction of glandular and squamous epithelium parts.  
499 Bar, 100  $\mu\text{m}$ . Panels C and D, Gram stain (C) and Wright-Giemsa stain (D) of sections of  
500 squamous epithelium. Bar, 100  $\mu\text{m}$ . Red arrowheads indicate gram-positive bacteria in a  
501 biofilm.

502 Staining of the sections of the fixed gastric tissue with Gram stain or Giemsa stain show a  
503 thick layer of gram-positive bacteria on the non-secretory epithelium portion of the stomach.  
504 This is similar to Savage et al. noted in the forestomachs of *M. musculus* (70). The appearance is  
505 also consistent with the *Lactobacillus* biofilm that was described by Wesney et al. (71).

506 Two of the species, “*L. peromysci*” and *L. animalis*, could reliably be distinguished by  
507 their distinctive colony morphologies from the isolated strains of *L. reuteri* and *L. johnsonii*,  
508 which had colonies of similar appearance (Fig 12). The rough-surfaced, ropy colonies of “*L.*  
509 *peromysci*” and the compact smooth colonies of *L. animalis* were similar to what Dubos and  
510 colleagues described in their study of lactobacilli of the mouse stomach and gut (72).

511 We next used a different set of 20 animals of the LL stock, 6 (2 females and 4 males) of  
512 which were born at the PGSC facility and 14 (7 females and 7 males) of which were born at U.C.  
513 Irvine. All animals were housed at U.C. Irvine for at least 26 weeks before euthanasia,  
514 dissection, and cultivation of the stomach tissue and contents.

515 **Fig 12.** Colonies and cells of lactobacilli of the *P. leucopus* stomach and gut. Panels A-C show  
516 representative sizes and morphologies of colonies of “*L. peromysci*”, *L. animalis*, and the less  
517 distinguishable *L. reuteri* and *L. johnsonii*. Bars, 1 mm. Panels D and E show magnified view of  
518 colonies of “*L. peromysci*” and *L. animalis* (D) and that of *L. reuteri* and *L. johnsonii* (E). Bar, 100  
519  $\mu\text{m}$ . Panel F, phase microscopy of wet mount of unconcentrated broth culture of “*L.*  
520 *peromysci*”. Bar, 10  $\mu\text{m}$ .

521 Mean (95% CI) colony forming units of lactobacilli per gram of stomach tissue on  
522 selective medium plates were ten-fold higher in females at  $7.4 (1.1-47.4) \times 10^9$  than in males at  
523  $0.76 (0.40-1.4) \times 10^9$  ( $t$ -test  $p = 0.02$  for log-transformed values) (Table 3). There was no  
524 discernible association with place of birth, and there was no difference between females and  
525 males in the proportions of the lactobacilli were identified as “*L. peromysci*”, *L. animalis*, and *L.*

526 *reuteri/L. johnsonii*. For five animals, whose lactobacilli were subjected to 16S ribosomal RNA  
 527 gene PCR and sequencing for confirmation, the *L. reuteri/L. johnsonii*-type colonies are  
 528 predominantly *L. reuteri*. But *L. johnsonii* was confirmed to be present as well and outnumbered  
 529 *L. reuteri* in one animal. The results for 3 animals that had been on a 9% fat content diet, which  
 530 was part of the breeding program, instead of 6% fat content were not distinguishable from those  
 531 for the other 17.

Table 3. Colony forming units (cfu) of *Lactobacillus* spp. in *Peromyscus leucopus* stomach

Animal ID	Sex	Log <sub>10</sub> total cfu/gm	% colony type		
			<i>animalis</i>	"peromysci"	<i>reuteri/johnsonii</i>
22403	F	10.9	3	32	65
22404	F	11.3	61	4	35
25053	F	10.7	37	60	3
25054	F	11.0	96	4	<1 <sup>a</sup>
25055	F	10.4	94	6	<1
25065	F	8.9	50	19	31
25062	F	8.5	60	14	26 (26/0) <sup>b</sup>
25063	F	8.8	52	12	36 (33/3)
25058	F	8.3	82	14	5 (5/0)
22401	M	8.6	33	19	48
22375	M	8.8	58	3	40
22420	M	9.7	48	19	33
22377	M	9.0	81	10	9
26050	M	8.4	87	6	7
25056	M	9.6	60	15	26



25010	M	9.0	84	16	<1
25060	M	8.8	55	23	23
25061	M	8.3	63	38	<1
25059	M	8.5	50	9	41 (36/5)
25011	M	9.0	61	24	14 (4/10)
Mean (95% CI)	n.a.	9.3 (8.9-9.8)	61 (51-70)	17 (11-23)	≤ 22

532 <sup>a</sup> <1, below limit of detection by serial dilution on plates

533 <sup>b</sup> ( / ), % *reuteri* / % *johnsonii* by PCR and 16S ribosomal rDNA sequencing

534 A separate group of 9 adult LL stock *P. leucopus* (5 females and 4 males) were euthanized  
535 after withholding food overnight, and the freshly-excised stomachs were subjected to DNA  
536 extraction without prior washing of the stomach. A mean (95% CI) of 477,688 (408,988-546,388)  
537 PE250 Illumina reads were obtained for the 9 samples (Table S7 of Supplementary information).  
538 These were mapped to the four *Lactobacillus* genomes as references, as described above, as well  
539 as to partial chromosomes for *Prevotella* sp. LL70 and *Helicobacter* sp. LL4 (Table 1). For an  
540 estimate of the number of mammalian nuclei represented in the stomach extract the *P. leucopus*  
541 genome (accession NMRJ000000000.1) served as the reference. Fig 13 shows the distributions of  
542 normalized reads mapping to the references as well as to the *P. leucopus* genome and  
543 cumulatively to all *Lactobacillus* spp. Females and males were similar by these measures for all  
544 these groups. For this group of animals and this analysis, we confirmed the high prevalence of  
545 “*L. peromysci*” in the stomach as well as the comparatively greater representation of *L. reuteri*  
546 over *L. johnsonii*. In this sample *L. animalis* was more variable in numbers between animals. As  
547 further evidence that the *Helicobacter* sp. was of the enterohepatic type, it was near undetectable

548 in the stomach extract, while a typically abundant genus in the intestine, *Prevotella*, was  
549 present in small numbers in some samples. The lactobacilli in the stomach were about as  
550 numerous as the stomach tissue cells constituting the sample.

551 **Fig 13.** Box-whisker plots of log-transformed normalized reads of total metagenomes of the  
552 stomachs of 9 *P. leucopus* (left panel) and *M. musculus* (right panel) that mapped to  
553 chromosomes of *Lactobacillus* spp. or other bacteria by host species and by sex. The references to  
554 which reads were mapped were complete chromosomes or partial chromosomes of organisms  
555 listed in Table 1. “*Lactobacillus*” in the first position of each panel were the cumulative reads for  
556 the four individual *Lactobacillus* species in this analysis.

557 A strain of *L. reuteri* was shown to be the source of biofilm in the GI tract of mice in one  
558 study (73), and *L. murinus*, the sister taxa of *L. animalis* (Fig 3), accounted for the biofilm in  
559 another study of the upper GI tract of *M. musculus* (74). *L. johnsonii* has also been demonstrated  
560 to produce an exopolysaccharide biofilm (75). In a study of germ-free mice in which bacteria  
561 were experimentally introduced, *L. taiwanensis*, which is in the same cluster as *L. johnsonii* and *L.*  
562 *gasseri* (67), formed a mixed-species biofilm with *L. reuteri* (76).

563 One limitation of this experiment is that we may have overlooked species that were not  
564 identified because they were not cultivable by our method and conditions, which were  
565 microaerophilic, not strictly anaerobic. That said, if cells of such non-cultivable lactobacilli had  
566 been present in the feces or stomach, their numbers did not reach a threshold for assembly into  
567 contigs of the de novo assembly of the high coverage sequencing and then detection.

## 568 **Gut metagenomes of a natural population**

569           The foregoing studies were of animals born and reared under controlled conditions,  
570 including the same diet and environmental parameters for all individuals in the group.  
571 Infectious diseases and predators were not a variable. The LL stock *P. leucopus* were outbred but  
572 the effective population size was small compared to a wild population (18). Which of our  
573 findings would hold for animals sampled in their native habitats?

574           This particular study of a natural population had two specific purposes. The first was to  
575 assess the species richness or alpha diversity of microbiota within a given animal and  
576 differences in species composition or beta diversity between animals. The second objective's  
577 question of whether any of the *Lactobacillus* species we identified in the stock colony were  
578 present in natural populations. For this survey we used fecal pellets from *P. leucopus* that were  
579 individually captured and then released on Block Island, several miles off-shore from the North  
580 American mainland. At time of capture the animals were identified as to species, sex, and stage  
581 of maturity.

582           We analyzed the data from fecal pellets of 18 different animals (10 females and 8 males),  
583 the majority of which were adults, collected from *P. leucopus* captured at different locations on  
584 Block Island (Table S14 of Supplementary information). As expected, there was greater variation  
585 between individual animals than was observed with the stock colony animals maintained under  
586 same conditions. Fig 10 compares the alpha diversity by Shannon index and beta diversity by

587 Bray-Curtis dissimilarity of the inbred BALB/c *M. musculus*, outbred LL stock *P. leucopus*, and  
588 the natural population of *P. leucopus* of Block Island.

589 By algorithmic assignment of reads to taxonomic family, *Lactobacillaceae* was one of the  
590 most prevalent bacteria with a mean of ~5% of reads, but this was over a range of 0.3% to 20%.  
591 As was the case for the stock colony *P. leucopus*, the frequency of *Helicobacteraceae* varied more  
592 widely between sampled animals than for comparably-prevalent taxa: a mean of ~1% but  
593 ranging from 0.03% to 12%. The frequency of a parabasalid protist, by the criterion of  
594 *Trichomonadidae* reads, in the metagenomes was similar to what we observed in the metagenome  
595 of the stock colony *P. leucopus*: the mean was 0.11% with a range of 0.02 to 0.62%. This was an  
596 indication that the *T. muris* was autochthonous in *P. leucopus*, but we did not have direct  
597 observation of the protozoa to confirm that.

598 Using the chromosome sequences of the four *Lactobacillus* species and partial  
599 chromosome sequences of *Spirochaetaceae* bacterium LL50, *Prevotella* sp. LL70, and *Helicobacter*  
600 sp. LL4 as references, we mapped and counted reads, as described for the LL stock and *M.*  
601 *musculus* study above. Fig 14 summarizes results for the 18 animals grouped by sex. Lactobacilli  
602 were common but, as seen with family level matching, there was greater variation between  
603 samples of the different animals than was observed for colony animals. There was also  
604 substantial variation in prevalences of the *Spirochaetaceae* bacterium and the *Prevotella* species. In  
605 most of the samples there was scant evidence of the *Helicobacter* species but in two animals,  
606 there were higher numbers of this organism, reaching 7% of the total reads in one fecal sample.

607 **Fig 14.** Box-whisker plots of log-transformed normalized reads of fecal metagenomes of 5  
608 female (red) and 4 male (blue) *P. leucopus* of a natural population of Block Island, Rhode Island.  
609 The reference genomes and other sequences were those described for Fig 13 and in addition the  
610 partial chromosome sequence of *Spirochaetaceae* sp. LL50. As an estimate of the number of  
611 mammalian cells in the extract, “nuclei” corresponded with normalized reads mapped to *P.*  
612 *leucopus* genome.

613         Among the lactobacilli used as references for this analysis, the two most prevalent  
614 species were “*L. peromysci*” and *L. animalis*. *L. reuteri* overall was about 10-fold lower in  
615 frequency, and *L. johnsonii* was about a hundred-fold lower in frequency. It is likely that reads  
616 called as *L. johnsonii* were the result of complete or partial matching to chromosomal loci that  
617 were highly conserved across the genus. Unlike the stock colony *P. leucopus* and the *M.*  
618 *musculus*, in this sampling of the Block Island population the samples from female animals had  
619 marginally lower representation of lactobacilli in the fecal samples than males.

620         To better characterize the two predominant *Lactobacillus* species in this set, we assembled  
621 contigs of reads mapping to “*L. peromysci*” or *L. animalis* from a higher coverage sequencing of  
622 the DNA of one of the Block Island samples. This yielded 51 of the 53 genes for ribosomal  
623 protein genes for a strain of *L. animalis*, which was designated 7442BI, and several core or  
624 housekeeping genes for the “*L. peromysci*”-like organism, which was designated BI7442 (Table  
625 1). Fig 15 shows phylograms of DNA sequences for these and related *Lactobacillus* species or  
626 strains. The concatenated sequence of the BI7442 isolate was 99.2% identical over the 11,252 nt

627 aligned with the corresponding sequences of the LL6 isolate of “*L. peromysci*”. Isolate 7442BI  
628 was comparatively more distant from the LL1 isolate of *L. animalis* in the stock colony but still  
629 clustered with it rather than with other examples of *L. animalis*.

630 **Fig 15.** Distance phylograms of concatenated codon-aligned nucleotide sequences of two  
631 *Lactobacillus* spp. of *P. leucopus* of Block Island, Rhode Island. Panel A, 10,152 positions of *ftsK*,  
632 *ftsZ*, *dnaA*, *dnaN*, *ileS*, and *topA* of “*L. peromysci*” LL6 and BI7442 and two other *Lactobacillus*  
633 species. Panel B, 18,552 positions of 51 of 53 ribosomal protein genes of six *L. animalis* strains,  
634 including LL1 and 7442BI. The distance criteria were Jukes-Cantor. The scales for distance are  
635 shown in each panel. Percent bootstrap (100 iterations) support values of  $\geq 80\%$  at a node are  
636 shown.

637         The sample size was limited, and we did not attempt culture isolations from the pellets.  
638 But the source of samples from *P. leucopus* was notable for its location on an island where *B.*  
639 *burgdorferi* is enzootic (77) and the risk of infection for residents and visitors is high (78). If there  
640 were to be future interventions targeting *P. leucopus* to interrupt disease transmission, Block  
641 Island would likely be a candidate site for this application.

642         This survey also documented that a strain or strains of “*L. peromysci*” and *L. animalis* are  
643 present in the native deermice. The high degree of sequence identity between two “*L.*  
644 *peromysci*” examples, whose origins were North Carolina and a New England island, long  
645 separated from the mainland, suggest that this newly-discovered species is autochthonous and  
646 plausibly a narrowly host-restricted symbiont of *P. leucopus*. Host-range restrictions of

647 lactobacilli for the stomachs of mice were demonstrated by Wesley and Tannock (71).  
648 Supporting an assignment of a symbiont lifestyle was its smaller genome size and lower % GC  
649 content of this species in comparison with *L. reuteri* and *L. johnsonii* with their broader host  
650 ranges (79).

## 651 **Conclusions**

652 Six decades ago René Dubos (of the epigraph), Russell Schaedler, and their colleagues at  
653 what is now Rockefeller University reported in a series of ground-breaking papers on the “fecal  
654 flora” of mice and variations in that microflora between mouse strains (80-82). They associated  
655 differences in gastrointestinal flora with growth rates of the mice and the mouse’s susceptibility  
656 to infection and endotoxin. A featured group of bacteria in their studies were lactobacilli. They  
657 showed that this group of bacteria were present in large numbers in the feces and that they  
658 predominated (up to  $10^9$  cfu per g of homogenate) in the stomachs of the mice (70), similarly to  
659 what we observed in *P. leucopus*. As their studies first intimated, the rodent may plausibly owe  
660 as much to the genomes of their microbiota as to the nuclei and mitochondria of their somatic  
661 cells for either ameliorating or exasperating disease (83).

662 There are also implications of our findings for development of oral vaccines that target *P.*  
663 *leucopus* to block transmission of pathogens either from tick to the reservoir or from the  
664 reservoir to the tick. Two of the candidate vehicles for the bait delivery of recombinant vaccine  
665 antigens to rodents have been *E. coli* and a *Lactobacillus* species (30, 84). In neither case were the

666 strains known to be adapted for life in *P. leucopus*. Success rate for achieving a protective  
667 response may be enhanced by use as the bacterial vehicle microbes that are adapted to *P.*  
668 *leucopus*. Such organisms presumably would more likely than an allochthonous bacterium to  
669 stably colonize and then proliferate to numbers large enough for the recombinant protein to  
670 elicit the sought-after immune responses.

671 Finally, this exploration and curation of microbes in the gut of the white-footed  
672 deer mouse concludes the third leg of our project on the total genome of representative animals  
673 of the species: the nuclear genome (18), the mitochondrial genome (17), and now the GI  
674 microbiome (85). This provides a foundation for testing of hypotheses by selective manipulation  
675 of the microbiota, for instance, by specifically targeting a certain species with a lytic phage or  
676 bacteriocin, to which it is not immune, and then evaluating the phenotype of the animal after  
677 this “knock-out”. Now that there is an annotated *P. leucopus* genome with millions of SNPs  
678 identified (UC Santa Cruz genome browser; <http://googl/LwHDr5>) it also feasible to investigate  
679 through forward genetics the host determinants of particular bacterial associations and for  
680 which there is evidence of variation within a population. An example would be the *Helicobacter*  
681 species that was highly variable in prevalence in both the wild animals and the stock colony  
682 animals.

## 683 **Materials and methods**

### 684 **Colony animals**



685 This study was carried out in strict accordance with the recommendations in the Guide  
686 for the Care and Use of Laboratory Animals of the National Institutes of Health. At the  
687 University of California Irvine protocol AUP-18-020 was approved by the Institutional Animal  
688 Care and Use Committee (IACUC)-approved protocol. Adult outbred *P. leucopus* of the LL stock  
689 were purchased from the Peromyscus Genetic Stock Center (PGSC) of the University of South  
690 Carolina (86). The closed colony of the LL stock was founded with 38 animals captured near  
691 Linville, NC in the mid-1980's. Some of the LL stock animals in the study were bred at the  
692 University of California Irvine's animal care facility from pairs originating at the PGSC. Adult  
693 BALB/cAnNCr1 (BALB/c) *M. musculus* were purchased from Charles River. For the species  
694 comparison experiment both the PGSC-bred *P. leucopus* and *M. musculus* animals were housed  
695 in Techniplast individual ventilated cages in vivarium rooms with a 12 hour-12 hours light-dark  
696 cycle, an ambient temperature of  $22 \pm 1$  °C, stable humidity, and on an ad libitum diet of 2020X  
697 Teklad global soy protein-free extruded rodent chow with 6% fat content (Envigo, Placentia,  
698 CA). Other animals of PGSC origin, including for the high-coverage gut metagenome study,  
699 were also housed under the same conditions and on the same diet. Twenty U.C. Irvine-bred  
700 animals were under the housing conditions and on the diet except for three (1 female and 2  
701 males) that were on 2019 Teklad global protein extruded rodent chow with 9% fat content.  
702 Before euthanasia with carbon dioxide asphyxiation and cervical dislocation and then dissection  
703 of the stomach, food but not water was withheld for 12 h for selected animals. *P. leucopus*  
704 studied at the PGSC were under IACUC-approved protocol 2349-101211-041917 of the  
705 University of South Carolina and were euthanized by isoflurane inhalation.

## 706 **Field site and animal trapping**

707           The study was performed under IACUC-approved protocol AC-AAAS6470 of Columbia  
708 University (77). Block Island, located 23 km from mainland Rhode Island, is part of the Outer  
709 Lands archipelagic region, which extends from Cape Cod, MA through to Staten Island, NY.  
710 Block Island is 25.2 sq. km, about 40% of which is maintained under natural conditions. The  
711 agent of Lyme disease *Borrelia burgdorferi* is enzootic on the island (87) Animals were trapped  
712 at three locations: 1, a nature conservation area (41.15694, -71.58972); 2, private land with  
713 woodlots and fields (41.16333, -71.56611); and 3, Block Island National Wildlife Refuge  
714 (41.21055, -71.57222). Trapping was carried out during the May-August period with Sherman  
715 live traps (H.B. Sherman Traps, Inc. Tallahassee, FL) that were baited with peanut butter, oats,  
716 and sunflower seeds. Traps were arranged in nine 200 m transects with one trap placed every 10  
717 m for a total of 180 traps at each location. Animals were removed from traps, weighed, sexed,  
718 and assessed as to age (adult, subadult, or juvenile) by pelage. Fecal pellets were collected and  
719 kept at -20 °C on site, during shipment and until DNA extraction. The species identification of  
720 the source of the fecal pellets as *P. leucopus* was confirmed by sequencing of the D-loop of the  
721 mitochondrion as described (17).

## 722 **Cultivation and enumeration of bacteria**

723           Lactobacilli were initially isolated and then propagated on Rogosa SL agar plates (Sigma-  
724 Aldrich) in candle jars at 37° C. Gram-negative bacteria and specifically *Escherichia coli* were

725 isolated and propagated on MacConkey Agar plates (Remel) incubated in ambient air at 37° C.  
726 For determinations of colony forming units (cfu) homogenates of stomach, cecum, or fecal  
727 pellets were suspended and the serially diluted in phosphate-buffer saline, pH 7.4, before  
728 plating in 100 µl volumes on solid media in 150 mm x 15 mm polystyrene Petri dishes. Colonies  
729 were counted manually. Liquid cultures of *Lactobacillus* spp. isolates or *E. coli* were in Difco  
730 Lactobacilli MRS Broth (Becton-Dickinson) or LB broth, respectively, and incubated at 37° C on  
731 a shaker. Bacteria were harvested by centrifugation at 8000 x g for 10 min. Antibiotic  
732 susceptibilities were determined by standard disk testing on Mueller-Hinton Agar (Sigma-  
733 Aldrich) plates and ciprofloxacin 5 µg, gentamicin 10 µg, ampicillin 10 µg, and  
734 sulfamethoxazole 23.75 – trimethoprim 1.25 µg BBL Sensi-Disc antibiotic disks (Becton-  
735 Dickinson) according the manufacturer instructions.

## 736 **Histology**

737 After the stomachs were removed from two euthanized *P. leucopus* LL stock adult  
738 females, they were opened longitudinally, gently flushed with PBS, and fixed in 10% buffered  
739 formalin (Thermo Fisher Scientific). Histological and histochemical analysis was performed on  
740 paraffin block sections of the stomach with Hematoxylin and Eosin, Wright-Giemsa and Gram  
741 stains (Abcam, Cambridge, UK).

## 742 **Microscopy, photography, and video**

743            Photographs of colonies on plates were taken with a Nikon Df DSLR camera and 60 mm  
744    Nikkor AF-S Micro lens with illumination by incident light above and reflected light below the  
745    plates on an Olympus SZ40 dissecting scope. An Olympus BX60 microscope with attached  
746    QIClick CCD camera and Q-Capture Pro7 software (Teledyne Photometrics, Tucson, AZ) was  
747    used for low-magnification images of colonies under bright light microscopy and 400X images  
748    under phase and differential interference microscopy. Histology slides were examined on a  
749    Leica DM 2500 microscope equipped with a MC120 HD digital camera (Leica Microsystems,  
750    Buffalo Grove, IL).

## 751    **DNA extractions**

752            DNA from fresh and frozen fecal pellets, from tissue of stomach and cecum, and from  
753    bacteria harvested from broth cultures were extracted with ZymoBIOMICS™ DNA Miniprep or  
754    Microprep kits (Zymo Research, Irvine, CA). Freshly-dissected, unwashed tissues were cut into  
755    small pieces before trituration and then homogenization in the lysis buffer. DNA concentration  
756    was determined by NanoDrop spectrophotometer and Qubit fluorometer (Thermo Fisher  
757    Scientific).

## 758    **PCR**

759            The near-complete 16S ribosomal RNA gene for *Lactobacillus* spp. was amplified using  
760    PCR using custom primers for the genus *Lactobacillus*: forward 5'-CCTAATACATGCAAGTCG  
761    and reverse 5'-GGTTCTCCTACGGCTA. The Platinum Taq polymerase and master mix

762 (ThermoFisher Scientific) contained uracil-DNA glycosylase. On a T100 thermal cycler (BioRad)  
763 PCR conditions (°C for temperature) The conditions were 37° for 10 min, 94° for min, 40 cycles  
764 of 94° for 10 s, 55° for 30 s, and 72° for 45 s. The 1.5 kb PCR product was isolated and purified  
765 from agarose gel using the NucleoSpin Gel and PCR Clean-up kit (Takara). The product was  
766 subjected to Sanger dideoxy sequencing at GENEWIZ (San Diego, CA).

## 767 **Whole genome sequencing, assembly, and annotation**

768 Long reads were obtained using an Oxford Nanopore Technology MinION Mk1B  
769 instrument with Ligation Sequencing Kit, R9.4.1 flow cell, MinKnow v. 19.6.8 for primary data  
770 acquisition, and Guppy v. 3.2.4 for base calling with default settings. Paired-end short reads  
771 were obtained on a MiSeq sequencer with paired-end v2 Micro chemistry and 150 cycles  
772 (Illumina, San Diego, CA). The library was constructed using the NEXTflex Rapid DNA-Seq kit  
773 (Bioo Scientific, Austin, TX), the quality of sequencing reads was analyzed using FastQC  
774 (Babraham Bioinformatics), and reads were trimmed of Phred scores <15 and corrected for poor-  
775 quality bases using Trimmomatic (88). A hybrid assembly was carried out with Unicycler v.0.4.7  
776 (89) with default settings and 16 threads on the High Performance Computing cluster of the  
777 University of California Irvine. Assembly of short reads alone were performed with the  
778 Assembly Cell program of CLC Genomics Workbench v. 11 (Qiagen). Annotation was provided  
779 by the NCBI Prokaryotic Genome Annotation Pipeline (90). Putative bacteriocins and their  
780 associated transport and immunity functions were identified by BAGEL4 (91, 92). For other  
781 analyses paired-end reads were mapped with a length fraction of 0.7 and similarity fraction of

782 0.9 to whole genomes sequences or concatenated large contigs representing partial genomes  
783 (Table 1). Mapped reads were normalized for length of reference sequence and for total reads  
784 after quality control and removal of adapters.

## 785 **Metagenome sequencing**

786 The library was constructed using NEXTflex Rapid DNA-Seq kit v2 (Bioo Scientific) and  
787 the NEXTflex Illumina DNA barcodes after shearing the DNA with a Covaris S220 instrument,  
788 end repair and adenylation, and clean-up of the reaction mixture with NEXTFLEX Clean Up  
789 magnetic beads (Beckman Coulter, Brea, CA). The library was quantified by qPCR with the  
790 Kapa Sybr Fast Universal kit (Kapa Biosystems, Woburn, MA), and the library size was  
791 determined by analysis using the Bioanalyzer 2100 DNA High Sensitivity Chip (Agilent  
792 Technologies). Multiplexed libraries were loaded on either an Illumina HiSeq 2500 sequencer  
793 (Illumina, San Diego, CA) with paired-end chemistry for 250 cycles or a MiSeq Sequencer  
794 (Illumina, San Diego, CA) with paired-end v2 Micro chemistry and 150 cycles. The Illumina real  
795 time analysis software RTA 1.18.54 converted the images into intensities and base calls. De novo  
796 assemblies were performed with De Novo Assembly v. 1.4 of CLC Genomics Workbench v. 11  
797 with the following settings: mismatch, insertion, and deletion costs of 3 each; length fraction of  
798 0.3, and similarity fraction of 0.93.

## 799 **16S ribosomal RNA analysis**

800 The same DNA extract used for the metagenome sequencing at University of California  
801 Irvine was submitted to ID Genomics, Inc. (Seattle, WA) and subjected the company's 16S rRNA  
802 Metagenomics service (<http://idgenomics.com/our-services>), which used the 16S Metagenomics  
803 v. 1.01 program (Illumina). Of the 333,358 reads 82%, were classified as to taxonomic family.

## 804 **Metagenome analysis**

805 Fastq files were uploaded to the metagenomic analysis server MG-RAST  
806 (<https://www.mg-rast.org>) (93). Reads were joined using join paired reads function on the  
807 browser and filtered for *Mus musculus* v37 genome. Artificial replicate sequences produced by  
808 sequencing artifacts were removed by the method of Gomez-Alvarez et al. (94). Low quality  
809 reads (Phred score <15 for no more than 5 bases) were removed using SolexQA, a modified  
810 DynamicTrim protocol (95). The output of the MG-RAST protocol was analyzed in R using the  
811 *vegan* package (<https://cran.r-project.org>, <https://github.com/vegandevs/vegan>). Alpha diversity  
812 was expressed by the Shannon's Diversity Index, which accounts for evenness as well as  
813 richness (96). Beta diversity expressed as the Bray-Curtis Dissimilarity statistic (97) was  
814 calculated using the *avgdist* function with 1000 sample depth, the median as the function, and  
815 100 iterations (<https://github.com/vegandevs/vegan/blob/master/man/avgdist.Rd>). Data was  
816 visualized using non-metric multidimensional scaling in two dimensions (98).  
817 MicrobiomeAnalyst (<https://www.microbiomeanalyst.ca>) (99) was used for hierarchical  
818 clustering by distance criterion and by means of Pearson correlations. The DFAST prokaryotic  
819 genome annotation pipeline (<https://dfast.nig.ac.jp>) was used for annotation of incomplete

820 chromosomes and large contigs (100). For *Lactobacillus* spp. and the *Helicobacter* sp. the lactic  
821 acid bacteria database and *Helicobacter* database, respectively, options were chosen. Alignments  
822 and phylogenetic analysis were carried out with the SeaView v. 4 suite (101).

## 823 **Data availability**

824 The resources for the several new sequences for genomes, large contigs, and individual  
825 genes that described here are listed in Table 1. The accession numbers for the annotated  
826 genomes and plasmids of *L. animalis* LL1, *L. reuteri* LL7, and “*L. peromysci*” LL6 are given in  
827 Bassam et al. (24). Fig 2 and its legend provides accession numbers for 16S ribosomal RNA gene  
828 sequences of other *Lactobacillus* species and strains. The nucleotide sequences of ribosomal  
829 proteins for different species and strains of *Lactobacillus* and *Helicobacter* were obtained from the  
830 Ribosomal MLST database of PubMLST (<https://pubmlst.org/rmlst/>) and given in Table S3 of  
831 Supplementary information. Additional accession numbers for individual genes of other  
832 organisms as references are given in Table S5 of Supplementary information. Hyperlinks to the  
833 long (Nanopore) and short (Illumina) sequence reads at the Sequence Read Archive or MG-  
834 RAST database are provided in Table 1 and Tables S7 and S13 of Supplementary information.

## 835 **Statistical analysis**

836 Normalized reads and other values whose distributions spanned more than one order of  
837 magnitude were log-transformed before parametric analysis by 2-tailed *t*-test. Inverse  
838 transformation was carried out to provide nonparametric means and corresponding asymmetric



839 95% confidence intervals. The  $Z$ -score was the number of standard deviations below or above  
840 the population mean a give raw value was. The False Discovery Rate (FDR) with corrected  $p$   
841 value was estimated by the method of Benjamini and Hochberg (102). The box-whisker plot  
842 graphs were made with SYSTAT v. 13.1 software (Systat Software, Inc.).

## 843 **Acknowledgements**

844 We thank Emma Keay and Vanessa Cook at the University of California Irvine and Asieh  
845 Naderi and Vimala Kaza at the University of South Carolina for their contributions to the study.  
846 The research was supported by National Institutes of Health grant R21 AI136523 to A.G.B.,  
847 National Science Foundation grants 1736150 and 1755670 to H. Kiaris (University of South  
848 Carolina), and National Science Foundation (Division of Integrative Organismal Systems) grant  
849 IOS1755286 to D.M.T. and M.A.D.

850

## 851 **References**

- 852 1. Dubos R. Autobiographical Manuscript. New York: Rockefeller University; 1981. p.  
853 Folder 14.
- 854 2. Sangodeyi F. Rene Dubos and the Emerging Science of Human Microbial Ecology New  
855 York: Rockefeller University; 2012 [<https://www.issuelab.org/resources/27965/27965.pdf>]

- 856 3. Hall ER. The Mammals of North America. Second ed. New York: John Wiley and Sons;  
857 1981.
- 858 4. Lackey JA, Huckaby DG, Ormiston BG. *Peromyscus leucopus*. Mammalian Species.  
859 1985(247):1-10.
- 860 5. Munshi-South J, Kharchenko K. Rapid, pervasive genetic differentiation of urban white-  
861 footed mouse (*Peromyscus leucopus*) populations in New York City. Mol Ecol. 2010.
- 862 6. Crossland JP, Dewey MJ, Barlow SC, Vrana PB, Felder MR, Szalai GJ. Caring for  
863 *Peromyscus* spp. in research environments. Lab Animal. 2014;43(5):162-6.
- 864 7. Kumar S, Stecher G, Suleski M, Hedges SB. TimeTree: a resource for timelines, timetrees,  
865 and divergence times. Mol Biol Evol. 2017;34:1812-9.
- 866 8. Stepan SJ, Schenk JJ. Muroid rodent phylogenetics: 900-species tree reveals increasing  
867 diversification rates. PLoS One. 2017;12(8):e0183070.
- 868 9. Schrago CG, Voloch CM. The precision of the hominid timescale estimated by relaxed  
869 clock methods. J Evol Biol. 2013;26(4):746-55.
- 870 10. Schug MD, Vessey SH, Korytko AI. Longevity and survival in a population of white-  
871 footed mice (*Peromyscus leucopus*). J Mammal. 1991;72:360-6.
- 872 11. Bunikis J, Tsao J, Luke CJ, Luna MG, Fish D, Barbour AG. *Borrelia burgdorferi* infection  
873 in a natural population of *Peromyscus leucopus* mice: a longitudinal study in an area where  
874 Lyme Borreliosis is highly endemic. J Infect Dis. 2004;189(8):1515-23.

- 875 12. Sacher G, Hart R. Longevity, aging, and comparative cellular and molecular biology of  
876 the house mouse, *Mus musculus*, and the white-footed mouse, *Peromyscus leucopus*. Birth  
877 Defects, Orig Artic Ser;(United States). 1978;14(1).
- 878 13. Shorter KR, Owen A, Anderson V, Hall-South AC, Hayford S, Cakora P, et al. Natural  
879 genetic variation underlying differences in *Peromyscus* repetitive and social/aggressive  
880 behaviors. Behavior Genet. 2014;44(2):126-35.
- 881 14. Veres M, Duselis AR, Graft A, Pryor W, Crossland J, Vrana PB, et al. The biology and  
882 methodology of assisted reproduction in deer mice (*Peromyscus maniculatus*). Theriogenology.  
883 2012;77(2):311-9.
- 884 15. Barbour AG. Infection resistance and tolerance in *Peromyscus* spp., natural reservoirs of  
885 microbes that are virulent for humans. Semin Cell Devel Biol. 2017;61(1):115-22.
- 886 16. Bedford NL, Hoekstra HE. *Peromyscus* mice as a model for studying natural variation.  
887 eLife. 2015;4:e06813.
- 888 17. Barbour AG, Shao H, Cook VJ, Baldwin-Brown J, Tsao JI, Long AD. Genomes, expression  
889 profiles, and diversity of mitochondria of the White-footed Deermouse *Peromyscus leucopus*,  
890 reservoir of Lyme disease and other zoonoses. Sci Rep. 2019;9(1):17618.
- 891 18. Long A, Baldwin-Brown J, Tao Y, Cook V, Balderrama-Gutierrez G, Corbett-Detig R, et  
892 al. The genome of *Peromyscus leucopus*, natural host for Lyme disease and other emerging  
893 infections. Sci Advances. 2019;5(7):eaaw6441.

- 894 19. Gomes-Solecki MJ, Brisson DR, Dattwyler RJ. Oral vaccine that breaks the transmission  
895 cycle of the Lyme disease spirochete can be delivered via bait. *Vaccine*. 2006;24(20):4440-9.
- 896 20. Najjar DA, Normandin AM, Strait EA, Esvelt KM. Driving towards ecotechnologies.  
897 *Pathogens Global Health*. 2017;111(8):448-58.
- 898 21. Specter M. Annals of Science: Rewriting the Code of Life. *The New Yorker*. 2017;93(1);  
899 January 2.
- 900 22. Baxter NT, Wan JJ, Schubert AM, Jenior ML, Myers P, Schloss PD. Intra- and  
901 interindividual variations mask interspecies variation in the microbiota of sympatric  
902 *peromyscus* populations. *Appl Environ Microbiol*. 2015;81(1):396-404.
- 903 23. Kohl KD, Dearing MD, Bordenstein SR. Microbial communities exhibit host species  
904 distinguishability and phyllosymbiosis along the length of the gastrointestinal tract. *Mol Ecol*.  
905 2018;27(8):1874-83.
- 906 24. Bassam K, Milovic A, Barbour AG. Genome sequences of three *Lactobacillus* species  
907 strains of the stomach of the White-footed Deermouse (*Peromyscus leucopus*). *Microbiol Res*  
908 *Announc*. 2019;8(40).
- 909 25. Herlemann DP, Geissinger O, Ikeda-Ohtsubo W, Kunin V, Sun H, Lapidus A, et al.  
910 Genomic analysis of "*Elusimicrobium minutum*," the first cultivated representative of the  
911 phylum "*Elusimicrobia*" (formerly termite group 1). *Appl Environ Microbiol*. 2009;75(9):2841-9.

- 912 26. Soo RM, Skennerton CT, Sekiguchi Y, Imelfort M, Paech SJ, Dennis PG, et al. An  
913 expanded genomic representation of the phylum Cyanobacteria. *Genome Biol Evol.*  
914 2014;6(5):1031-45.
- 915 27. Falony G, Joossens M, Vieira-Silva S, Wang J, Darzi Y, Faust K, et al. Population-level  
916 analysis of gut microbiome variation. *Science.* 2016;352(6285):560-4.
- 917 28. Walter J. Ecological role of lactobacilli in the gastrointestinal tract: implications for  
918 fundamental and biomedical research. *Appl Environ Microbiol.* 2008;74(16):4985-96.
- 919 29. Tannock G. The microecology of lactobacilli inhabiting the gastrointestinal tract. In:  
920 Marshall KC, editor. *Advances in Microbial Ecology.* 11. Boston, MA: Springer; 1990. p. 147-71.
- 921 30. Gomes-Solecki M, Richer L. Recombinant *E. coli* dualistic role as an antigen-adjuvant  
922 delivery vehicle for oral immunization. In: Pal U, Buyuktanir O, editors. *Borrelia burgdorferi*  
923 *Methods in Molecular Biology.* New York: Humana Press; 2018. p. 347-57.
- 924 31. Jolley KA, Bliss CM, Bennett JS, Bratcher HB, Brehony C, Colles FM, et al. Ribosomal  
925 multilocus sequence typing: universal characterization of bacteria from domain to strain.  
926 *Microbiology.* 2012;158(Pt 4):1005-15.
- 927 32. Fujisawa T, Itoh K, Benno Y, Mitsuoka T. *Lactobacillus intestinalis* (ex Hemme 1974) sp.  
928 nov., nom. rev., isolated from the intestines of mice and rats. *Int J Syst Bacteriol.* 1990;40(3):302-  
929 4.

- 930 33. Kim D, Cho MJ, Cho S, Lee Y, Byun SJ, Lee S. Complete Genome Sequence of  
931 *Lactobacillus reuteri* Byun-re-01, isolated from mouse small intestine. *Microbiol Res Announc.*  
932 2018;7(17).
- 933 34. Sun Z, Harris HM, McCann A, Guo C, Argimon S, Zhang W, et al. Expanding the  
934 biotechnology potential of lactobacilli through comparative genomics of 213 strains and  
935 associated genera. *Nat Commun.* 2015;6:8322.
- 936 35. Dent V, Williams R. *Lactobacillus animalis* sp. nov., a new species of *Lactobacillus* from  
937 the alimentary canal of animals. *Zentralblatt für Bakteriologie Mikrobiologie und Hygiene: I*  
938 *Abt Originale C: Allgemeine, angewandte und ökologische Mikrobiologie.* 1982;3(3):377-86.
- 939 36. Nam SH, Choi SH, Kang A, Kim DW, Kim RN, Kim A, et al. Genome sequence of  
940 *Lactobacillus animalis* KCTC 3501. *J Bacteriol.* 2011;193(5):1280-1.
- 941 37. Claesson MJ, Li Y, Leahy S, Canchaya C, van Pijkeren JP, Cerdeno-Tarraga AM, et al.  
942 Multireplicon genome architecture of *Lactobacillus salivarius*. *Proc Natl Acad Sci U S A.*  
943 2006;103(17):6718-23.
- 944 38. Frese SA, Benson AK, Tannock GW, Loach DM, Kim J, Zhang M, et al. The evolution of  
945 host specialization in the vertebrate gut symbiont *Lactobacillus reuteri*. *PLoS Genet.*  
946 2011;7(2):e1001314.

- 947 39. Bandara M, Skehel JM, Kadioglu A, Collinson I, Nobbs AH, Blocker AJ, et al. The  
948 accessory Sec system (SecY2A2) in *Streptococcus pneumoniae* is involved in export of  
949 pneumolysin toxin, adhesion and biofilm formation. *Microbes Infect.* 2017;19(7-8):402-12.
- 950 40. Denou E, Pridmore RD, Berger B, Panoff J-M, Arigoni F, Brüssow H. Identification of  
951 genes associated with the long-gut-persistence phenotype of the probiotic *Lactobacillus*  
952 *johnsonii* strain NCC533 using a combination of genomics and transcriptome analysis. *J*  
953 *Bacteriol.* 2008;190(9):3161-8.
- 954 41. Wilson CM, Aggio RB, O'Toole PW, Villas-Boas S, Tannock GW. Transcriptional and  
955 metabolomic consequences of LuxS inactivation reveal a metabolic rather than quorum-sensing  
956 role for LuxS in *Lactobacillus reuteri* 100-23. *J Bacteriol.* 2012;194(7):1743-6.
- 957 42. Hidalgo-Cantabrana C, Goh YJ, Pan M, Sanozky-Dawes R, Barrangou R. Genome editing  
958 using the endogenous type I CRISPR-Cas system in *Lactobacillus crispatus*. *Proc Natl Acad Sci*  
959 *U S A.* 2019;116(32):15774-83.
- 960 43. Saulnier DM, Santos F, Roos S, Mistretta TA, Spinler JK, Molenaar D, et al. Exploring  
961 metabolic pathway reconstruction and genome-wide expression profiling in *Lactobacillus*  
962 *reuteri* to define functional probiotic features. *PLoS One.* 2011;6(4):e18783.
- 963 44. Moreno-Vivian C, Cabello P, Martinez-Luque M, Blasco R, Castillo F. Prokaryotic nitrate  
964 reduction: molecular properties and functional distinction among bacterial nitrate reductases. *J*  
965 *Bacteriol.* 1999;181(21):6573-84.

- 966 45. Hwang H, Lee JH. Characterization of arginine catabolism by lactic acid bacteria isolated  
967 from kimchi. *Molecules* (Basel, Switzerland). 2018;23(11).
- 968 46. Singer JR, Blosser EG, Zindl CL, Silberger DJ, Conlan S, Laufer VA, et al. Preventing  
969 dysbiosis of the neonatal mouse intestinal microbiome protects against late-onset sepsis. *Nat*  
970 *Med*. 2019;25(11):1772-82.
- 971 47. Peña JA, Li SY, Wilson PH, Thibodeau SA, Szary AJ, Versalovic J. Genotypic and  
972 phenotypic studies of murine intestinal lactobacilli: species differences in mice with and without  
973 colitis. *Appl Environ Microbiol*. 2004;70(1):558-68.
- 974 48. Sheh A, Shen Z, Fox JG. Draft genome sequences of eight enterohepatic *Helicobacter*  
975 species isolated from both laboratory and wild rodents. *Genome Announc*. 2014;2(6).
- 976 49. Suerbaum S, Josenhans C, Sterzenbach T, Drescher B, Brandt P, Bell M, et al. The  
977 complete genome sequence of the carcinogenic bacterium *Helicobacter hepaticus*. *Proc Natl*  
978 *Acad Sci U S A*. 2003;100(13):7901-6.
- 979 50. Fox JG, Ge Z, Whary MT, Erdman SE, Horwitz BH. *Helicobacter hepaticus* infection in  
980 mice: models for understanding lower bowel inflammation and cancer. *Mucosal Immunol*.  
981 2011;4(1):22-30.
- 982 51. Bracken TC, Cooper CA, Ali Z, Truong H, Moore JM. *Helicobacter* infection significantly  
983 alters pregnancy success in laboratory mice. *J Am Assoc Lab Animal Sci*. 2017;56(3):322-9.



- 984 52. Nordhoff M, Taras D, Macha M, Tedin K, Busse HJ, Wieler LH. *Treponema berlinense* sp.  
985 nov. and *Treponema porcinum* sp. nov., novel spirochaetes isolated from porcine faeces. *Int J*  
986 *Syst Evol Microbiol.* 2005;55(Pt 4):1675-80.
- 987 53. Barbour AG. *Borreliaceae*. In: Whitman WB, Rainey R, P. Kämpfe P, Trujillo M, Chun J,  
988 DeVos P, et al., editors. *Bergey's Manual of Systematics of Archaea and Bacteria*. 2018. p. 1-9.
- 989 54. Geissinger O, Herlemann DP, Morschel E, Maier UG, Brune A. The ultramicrobacterium  
990 "*Elusimicrobium minutum*" gen. nov., sp. nov., the first cultivated representative of the termite  
991 group 1 phylum. *Appl Environ Microbiol.* 2009;75(9):2831-40.
- 992 55. Lagkouvardos I, Lesker TR, Hitch TCA, Galvez EJC, Smit N, Neuhaus K, et al. Sequence  
993 and cultivation study of Muribaculaceae reveals novel species, host preference, and functional  
994 potential of this yet undescribed family. *Microbiome.* 2019;7(1):28.
- 995 56. Doran DJ. A catalogue of the protozoa and helminths of North American rodents. I.  
996 Protozoa and Acanthocephala. *Am Midland Naturalist.* 1954;52(1):118-28.
- 997 57. Ericsson AC, Gagliardi J, Bouhan D, Spollen WG, Givan SA, Franklin CL. The influence  
998 of caging, bedding, and diet on the composition of the microbiota in different regions of the  
999 mouse gut. *Sci Rep.* 2018;8(1):4065.
- 1000 58. Steiner JM, Schwamberger S, Pantchev N, Balzer HJ, Vrhovec MG, Lesina M, et al. Use of  
1001 ronidazole and limited culling to eliminate *Tritrichomonas muris* from laboratory mice. *J Am*  
1002 *Assoc Lab Animal Sci.* 2016;55(4):480-3.

- 1003 59. Koyama T, Endo T, Asahi H, Kuroki T. Life cycle of *Tritrichomonas muris*. Zentralblatt  
1004 für Bakteriologie, Mikrobiologie und Hygiene Series A: Medical Microbiology, Infectious  
1005 Diseases, Virology, Parasitology. 1987;264(3-4):478-86.
- 1006 60. Hackstein JH, Akhmanova A, Boxma B, Harhangi HR, Voncken FG. Hydrogenosomes:  
1007 eukaryotic adaptations to anaerobic environments. Trends Microbiol. 1999;7(11):441-7.
- 1008 61. Rae DO, Crews JE. *Tritrichomonas foetus*. Vet Clin North Am Food Animal Practice.  
1009 2006;22(3):595-611.
- 1010 62. Yao C, Koster LS. *Tritrichomonas foetus* infection, a cause of chronic diarrhea in the  
1011 domestic cat. Vet Res. 2015;46:35.
- 1012 63. Escalante NK, Lemire P, Cruz Tleugabulova M, Prescott D, Mortha A, Streutker CJ, et al.  
1013 The common mouse protozoa *Tritrichomonas muris* alters mucosal T cell homeostasis and  
1014 colitis susceptibility. J Exp Med. 2016;213(13):2841-50.
- 1015 64. Howitt MR, Lavoie S, Michaud M, Blum AM, Tran SV, Weinstock JV, et al. Tuft cells,  
1016 taste-chemosensory cells, orchestrate parasite type 2 immunity in the gut. Science.  
1017 2016;351(6279):1329-33.
- 1018 65. Chudnovskiy A, Mortha A, Kana V, Kennard A, Ramirez JD, Rahman A, et al. Host-  
1019 rotozoan interactions protect from mucosal infections through activation of the inflammasome.  
1020 Cell. 2016;167(2):444-56.e14.

- 1021 66. Lange BM, Croteau R. Isopentenyl diphosphate biosynthesis via a mevalonate-  
1022 independent pathway: Isopentenyl monophosphate kinase catalyzes the terminal enzymatic  
1023 step. *Proc Natl Acad Sci USA*. 1999;96(24):13714-9.
- 1024 67. Hammes WP, Vogel RF. The genus *Lactobacillus*. In: Wood B, Holzapfel W, editors. *The*  
1025 *Genera of Lactic Acid Bacteria*: Springer; 1995. p. 19-54.
- 1026 68. Salzman NH, de Jong H, Paterson Y, Harmsen HJM, Welling GW, Bos NA. Analysis of  
1027 16S libraries of mouse gastrointestinal microflora reveals a large new group of mouse intestinal  
1028 bacteria. *Microbiol*. 2002;148(Pt 11):3651-60.
- 1029 69. Carleton MD. A survey of gross stomach morphology in New World Cricetinae  
1030 (Rodentia, Muroidea), with comments on functional interpretations. *Miscellaneous Publications,*  
1031 *University of Michigan No 1461973*.
- 1032 70. Savage DC, Dubos R, Schaedler RW. The gastrointestinal epithelium and its  
1033 autochthonous bacterial flora. *J Exp Med*. 1968;127(1):67-76.
- 1034 71. Wesney E, Tannock GW. Association of rat, pig, and fowl biotypes of lactobacilli with the  
1035 stomach of gnotobiotic mice. *Microbial Ecol*. 1979;5(1):35-42.
- 1036 72. Dubos R, Schaedler RW, Costello R, Hoet P. Indigenous, normal, and autochthonous  
1037 flora of the gastrointestinal tract *J Exp Med*. 1965;122:67-76.
- 1038 73. Salas-Jara MJ, Ilabaca A, Vega M, Garcia A. Biofilm forming *Lactobacillus*: new  
1039 challenges for the development of probiotics. *Microorganisms*. 2016;4(3).

- 1040 74. Almiron M, Traglia G, Rubio A, Sanjuan N. Colonization of the mouse upper  
1041 gastrointestinal tract by *Lactobacillus murinus*: a histological, immunocytochemical, and  
1042 ultrastructural study. *Curr Microbiol.* 2013;67(4):395-8.
- 1043 75. Dertli E, Mayer MJ, Narbad A. Impact of the exopolysaccharide layer on biofilms,  
1044 adhesion and resistance to stress in *Lactobacillus johnsonii* FI9785. *BMC Microbiol.* 2015;15:8.
- 1045 76. Lin XB, Wang T, Stothard P, Corander J, Wang J, Baines JF, et al. The evolution of  
1046 ecological facilitation within mixed-species biofilms in the mouse gastrointestinal tract. *ISME J.*  
1047 2018;12(11):2770-84.
- 1048 77. Huang CI, Kay SC, Davis S, Tufts DM, Gaffett K, Tefft B, et al. High burdens of *Ixodes*  
1049 *scapularis* larval ticks on white-tailed deer may limit Lyme disease risk in a low biodiversity  
1050 setting. *Ticks Tick Borne Dis.* 2019;10(2):258-68.
- 1051 78. Finch C, Al-Damluji MS, Krause PJ, Niccolai L, Steeves T, O'Keefe CF, et al. Integrated  
1052 assessment of behavioral and environmental risk factors for Lyme disease infection on Block  
1053 Island, Rhode Island. *PLoS One.* 2014;9(1):e84758.
- 1054 79. Moran NA, McCutcheon JP, Nakabachi A. Genomics and evolution of heritable bacterial  
1055 symbionts. *Annu Rev Genet.* 2008;42:165-90.
- 1056 80. Dubos R, Schaedler RW. Some biological effects of the digestive flora. *Am J Med Sci.*  
1057 1962;244:265-71.

- 1058 81. Dubos RJ, Schaedler RW. The effect of diet on the fecal bacterial flora of mice and on their  
1059 resistance to infection. *J Exp Med*. 1962;115:1161-72.
- 1060 82. Schaedler RW, Dubos RJ. The fecal flora of various strains of mice. Its bearing on their  
1061 susceptibility to endotoxin. *J Exp Med*. 1962;115:1149-60.
- 1062 83. Rosshart SP, Vassallo BG, Angeletti D, Hutchinson DS, Morgan AP, Takeda K, et al. Wild  
1063 mouse gut microbiota promotes host fitness and improves disease resistance. *Cell*.  
1064 2017;171(5):1015-28.e13.
- 1065 84. Del Rio B, Seegers JF, Gomes-Solecki M. Immune response to *Lactobacillus plantarum*  
1066 expressing *Borrelia burgdorferi* OspA is modulated by the lipid modification of the antigen.  
1067 *PLoS One*. 2010;5(6):e11199.
- 1068 85. Carroll IM, Threadgill DW, Threadgill DS. The gastrointestinal microbiome: a malleable,  
1069 third genome of mammals. *Mamm Genome*. 2009;20(7):395-403.
- 1070 86. *Peromyscus* Genetic Stock Center. *Peromyscus* Genetic Stock Center, Columbia, SC:  
1071 University of South Carolina; 2017 [Available from: <http://stkctr.biol.sc.edu>].
- 1072 87. Tufts DM, Diuk-Wasser MA. Transplacental transmission of tick-borne *Babesia microti* in  
1073 its natural host *Peromyscus leucopus*. *Parasit Vectors*. 2018;11(1):286.
- 1074 88. Bolger AM, Lohse M, Usadel B. Trimmomatic: a flexible trimmer for Illumina sequence  
1075 data. *Bioinformatics*. 2014:btu170.

- 1076 89. Wick RR, Judd LM, Gorrie CL, Holt KE. Unicycler: Resolving bacterial genome  
1077 assemblies from short and long sequencing reads. *PLoS Comput Biol.* 2017;13(6):e1005595. doi:  
1078 10.1371/journal.pcbi.1005595.
- 1079 90. Haft DH, DiCuccio M, Badretdin A, Brover V, Chetvernin V, O'Neill K, et al. RefSeq: an  
1080 update on prokaryotic genome annotation and curation. *Nucl Acids Res.* 2018;46(D1):D851-d60.
- 1081 91. de Jong A, van Heel AJ. BAGEL4 Groningen, the Netherlands: University of Groningen;  
1082 2019 [Available from: <http://bagel4.molgenrug.nl>].
- 1083 92. van Heel AJ, de Jong A, Song C, Viel JH, Kok J, Kuipers OP. BAGEL4: a user-friendly  
1084 web server to thoroughly mine RiPPs and bacteriocins. *Nucl Acids Res.* 2018;46(W1):W278-W81.
- 1085 93. Meyer F, Paarmann D, D'Souza M, Olson R, Glass EM, Kubal M, et al. The metagenomics  
1086 RAST server – a public resource for the automatic phylogenetic and functional analysis of  
1087 metagenomes. *BMC Bioinformatics.* 2008;9(1):386.
- 1088 94. Gomez-Alvarez V, Teal TK, Schmidt TM. Systematic artifacts in metagenomes from  
1089 complex microbial communities. *ISME J.* 2009;3(11):1314-7.
- 1090 95. Cox MP, Peterson DA, Biggs PJ. SolexaQA: At-a-glance quality assessment of Illumina  
1091 second-generation sequencing data. *BMC Bioinformatics.* 2010;11(1):485.
- 1092 96. Hill MO. Diversity and evenness: a unifying notation and its consequences. *Ecology.*  
1093 1973;54(2):427-32.

- 1094 97. Bray JR, Curtis JT. An ordination of the upland forest communities of southern  
1095 Wisconsin. *Ecological Monographs*. 1957;27(4):325-49.
- 1096 98. Ward JH. Hierarchical grouping to optimize an objective function. *J Am Stat Assoc*.  
1097 1963;58(301):236-44.
- 1098 99. Chong J, Liu P, Zhou G, Xia J. Using MicrobiomeAnalyst for comprehensive statistical,  
1099 functional, and meta-analysis of microbiome data. *Nature Protocols*. 2020;15(3):799-821.
- 1100 100. Tanizawa Y, Fujisawa T, Nakamura Y. DFAST: a flexible prokaryotic genome annotation  
1101 pipeline for faster genome publication. *Bioinformatics*. 2017;34(6):1037-9.
- 1102 101. Gouy M, Guindon S, Gascuel O. SeaView version 4: A multiplatform graphical user  
1103 interface for sequence alignment and phylogenetic tree building. *Mol Biol Evol*. 2010;27(2):221-4.
- 1104 102. Benjamini Y, Hochberg Y. Controlling the false discovery rate: a practical and powerful  
1105 approach to multiple testing. *J Royal Stat Soc Series B (Methodological)*. 1995:289-300.
- 1106

## Supporting information

**Fig S1. Rarefaction curve for high-coverage sequencing of *Peromyscus leucopus* LL stock gut metagenome.**

**Fig S2. MG-RAST analysis high-coverage sequencing of *Peromyscus leucopus* LL stock gut metagenome by phylum.**

**Fig S2. MG-RAST analysis high-coverage sequencing of *Peromyscus leucopus* LL stock gut metagenome by subsystems.**

**Fig S4. Maximum likelihood phylogram of 470 aligned amino acids of DNA polymerase type B, organellar and viral family protein of *Tritrichomonas* sp. LL5 (Table 1) and homologous proteins of other protozoa (*T. foetus*, *Trichomonas vaginalis*, *Entamoeba invadens*, and *Giardia* sp.), oocytes (*Aphanomyces astaci* and *Thraustotheca clavata*), and bacteria (Division WS6 bacterium and *Haliea* sp.).** The GenBank accession numbers for the sequences are given next to organism name. The bootstrapped tree was generated with PhyML with the settings of the LG model, 4 rate classes, and 100 replicates.

**Table S1. Comparison of 16S sequence-based and metagenome-based identification of bacterial families in fecal pellets of LL stock *P. leucopus***

**Table S2. Metagenome by taxonomic family of fecal pellets of LL stock *P. leucopus***



- 1125 **Table S3. Sources of coding sequences for ribosomal proteins at rMLST database of**  
1126 <http://mlst.org>
- 1127 **Table S4. Putative bacteriocins and associated transport proteins and immunity proteins of 3**  
1128 *Lactobacillus* species of *Peromyscus leucopus*
- 1129 **Table S5. Accession numbers of sequences of other species**
- 1130 **Table S6. Statistics for gut metagenomes of *Peromyscus leucopus* and *Mus musculus***
- 1131 **Table S7. *Peromyscus leucopus* and *Mus musculus* gut metagenome accession numbers**
- 1132 **Table S8. Replicates of libraries of *Peromyscus leucopus* DNA extracts of fecal pellets**
- 1133 **Table S9. Log<sub>10</sub> of mean number of normalized reads for gut metagenomes of *Peromyscus***  
1134 *leucopus* and *Mus musculus* by families with >3000 reads
- 1135 **Table S10. Log<sub>10</sub> of reads matched to function for metagenomes of fecal pellets of**  
1136 *Peromyscus leucopus* and *Mus musculus*
- 1137 **Table S11. Map-to-reference normalized PE250 reads (log<sub>10</sub>) for feces and stomach sample**  
1138 **against *Lactobacillus* spp. and selected other bacteria**
- 1139 **Table S12. Comparison of gut metagenomes of *Peromyscus leucopus* and *Mus musculus* by**  
1140 **KEGG orthology gene**
- 1141 **Table S13. Reads of gut metagenomes of *Peromyscus leucopus* and *Mus musculus* by KEGG**  
1142 **orthology gene for individual animals and data for analysis of Table S11**

1143 **Table S14. Block Island *Peromyscus leucopus* fecal metagenome**

1144 **Movie S1. Cecal content with *Tritrichomonas* flagellates**

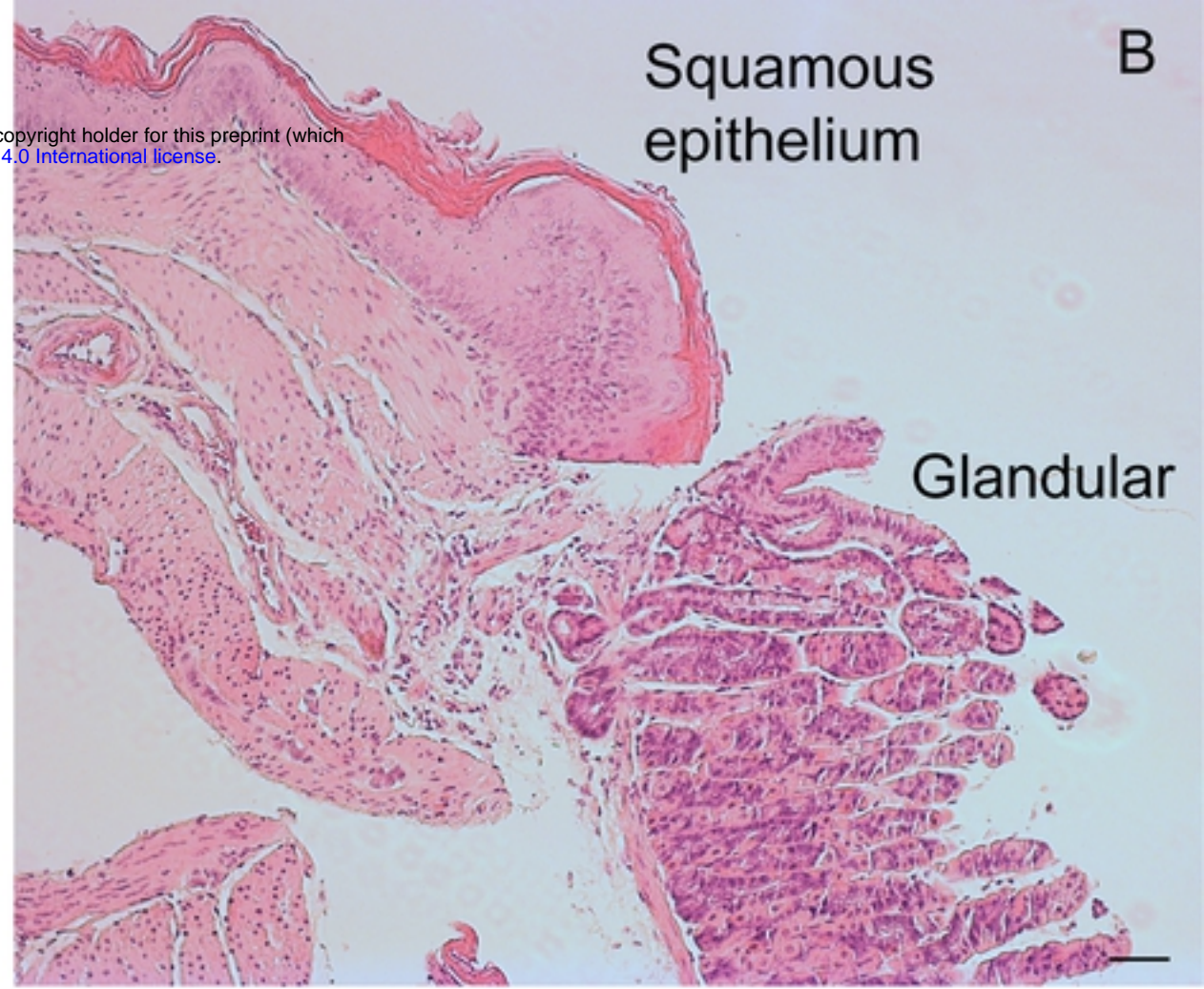


**A** Forestomach

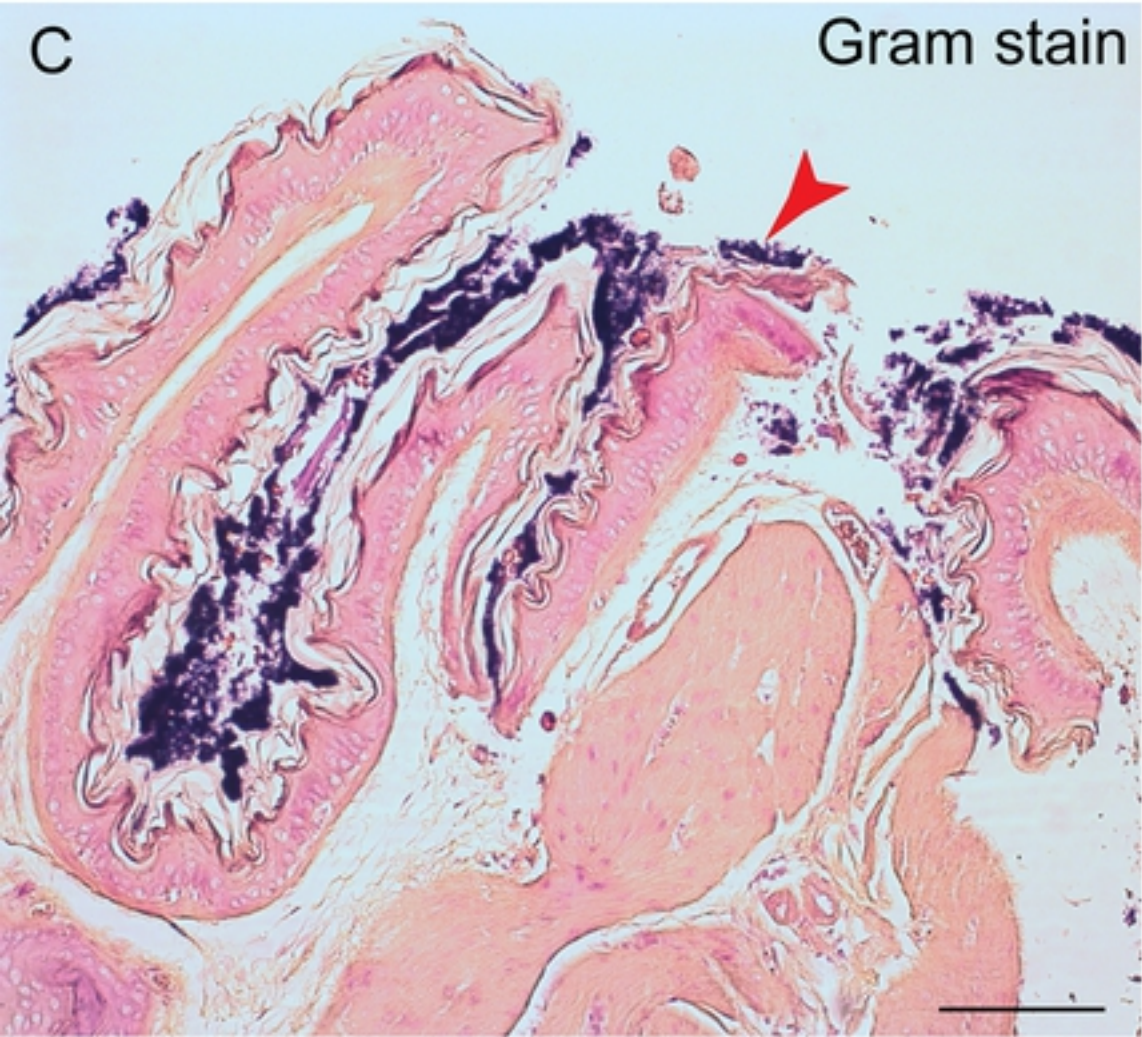


bioRxiv preprint doi: <https://doi.org/10.1101/2020.04.02.021659>; this version posted April 2, 2020. The copyright holder for this preprint (which was not certified by peer review) is the author/funder. It is made available under a [CC-BY 4.0 International license](https://creativecommons.org/licenses/by/4.0/).

**B** Squamous epithelium



**C** Gram stain



**D** Giemsa stain

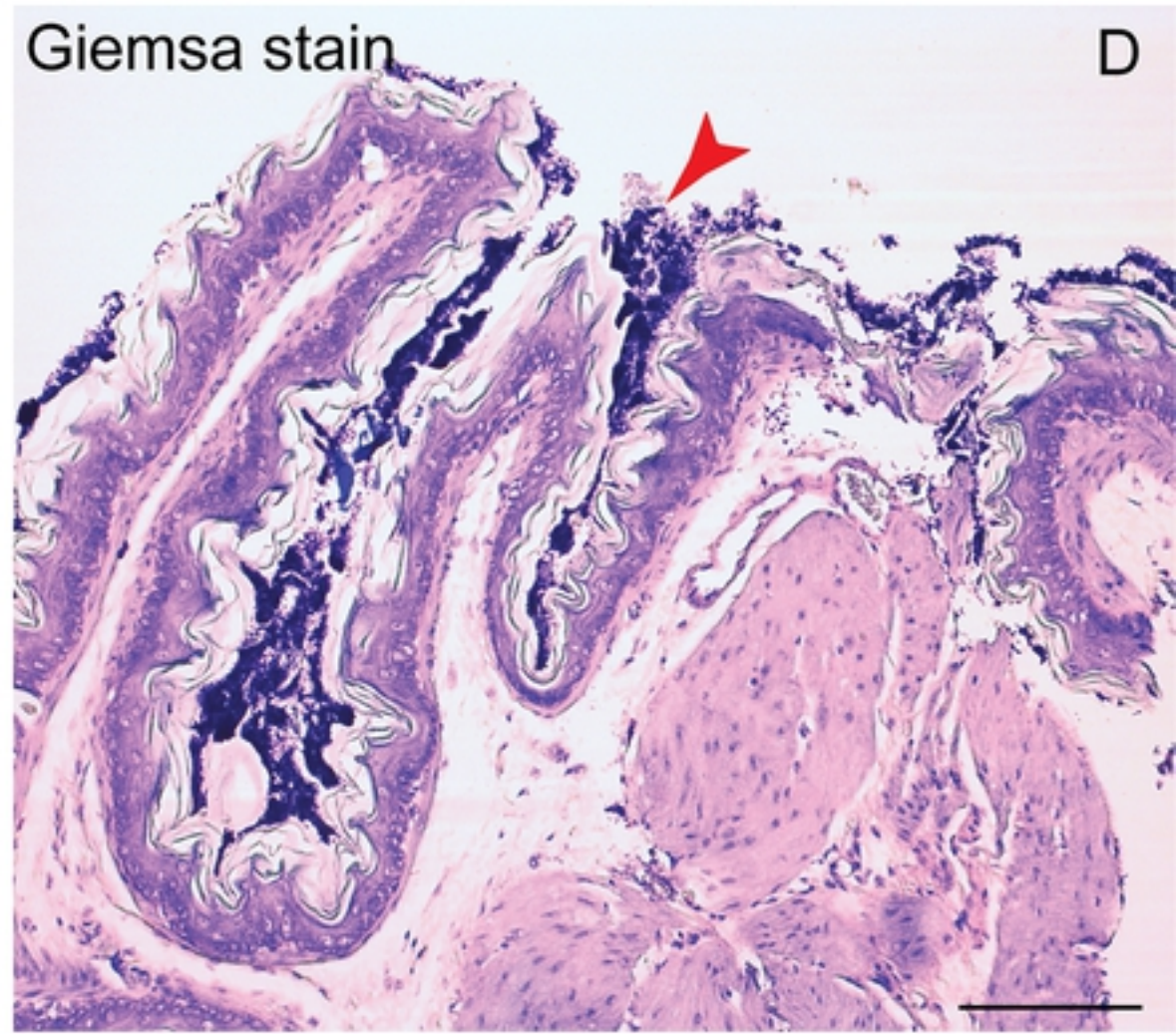


**Figure 11**



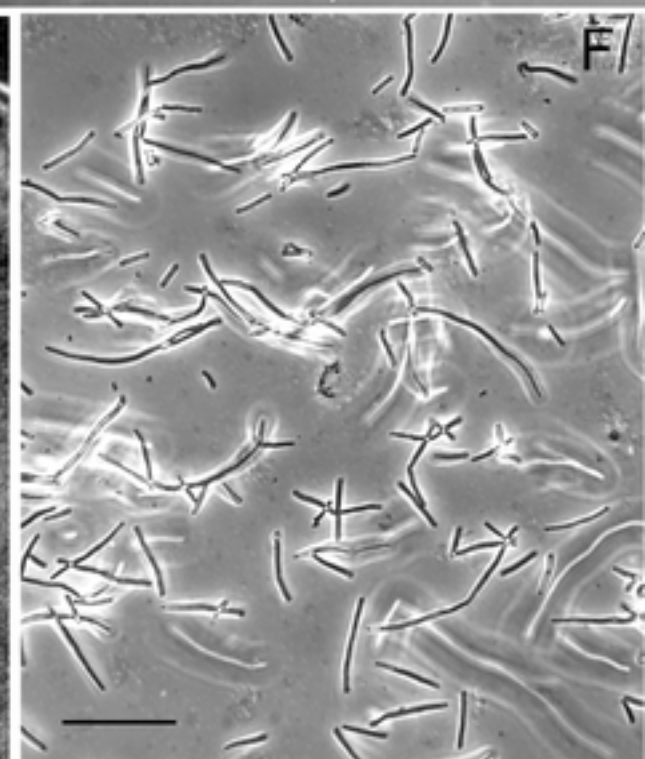
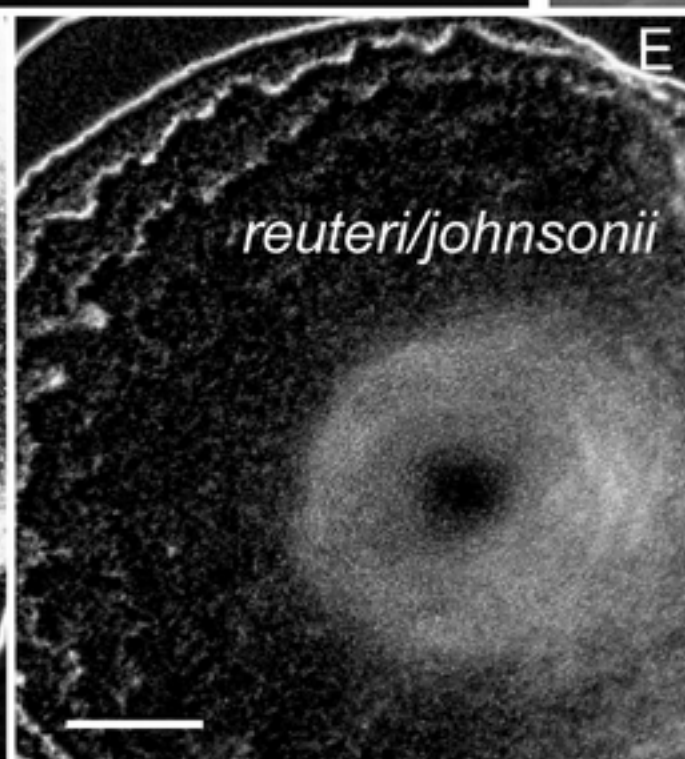
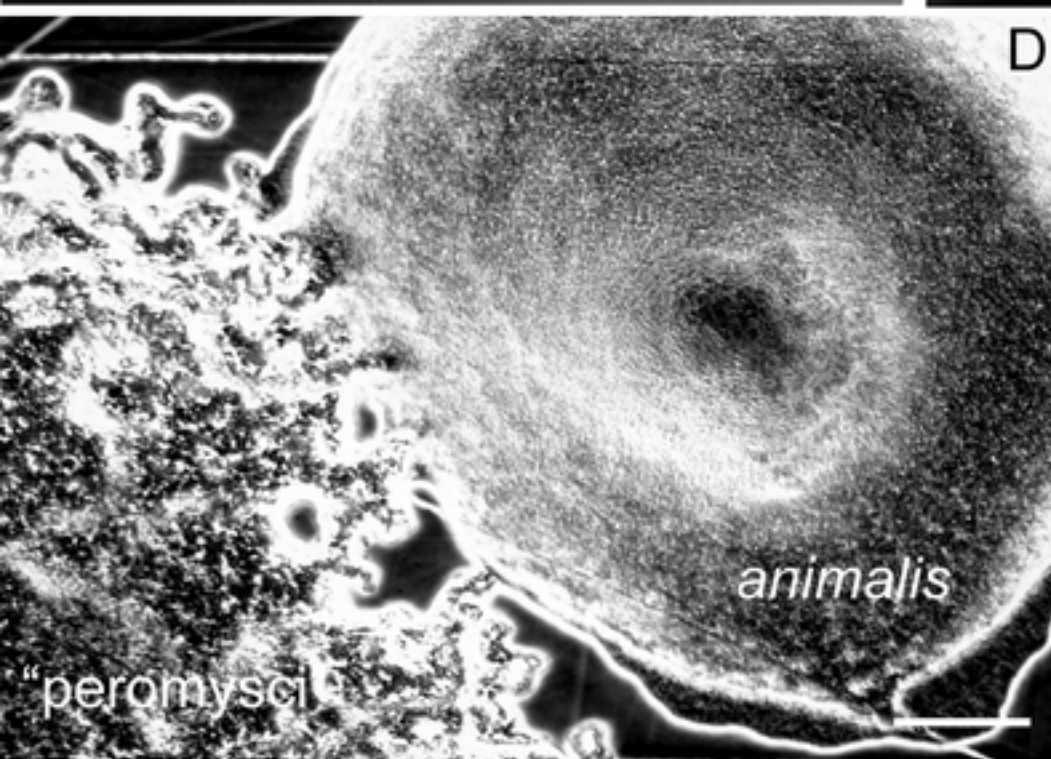
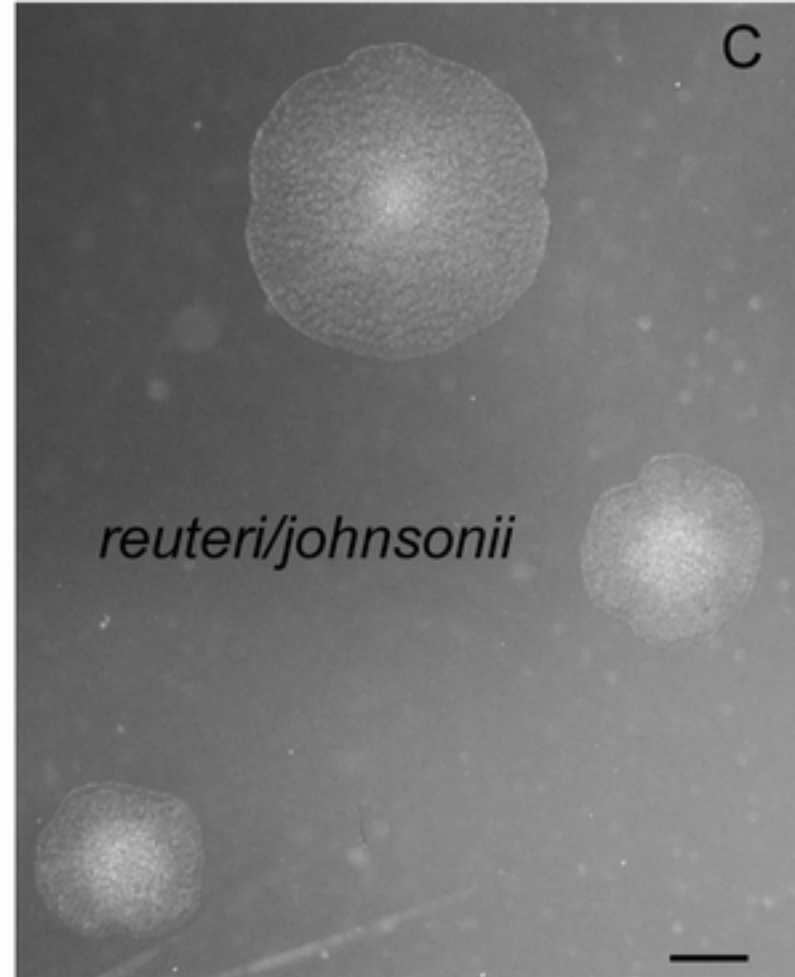
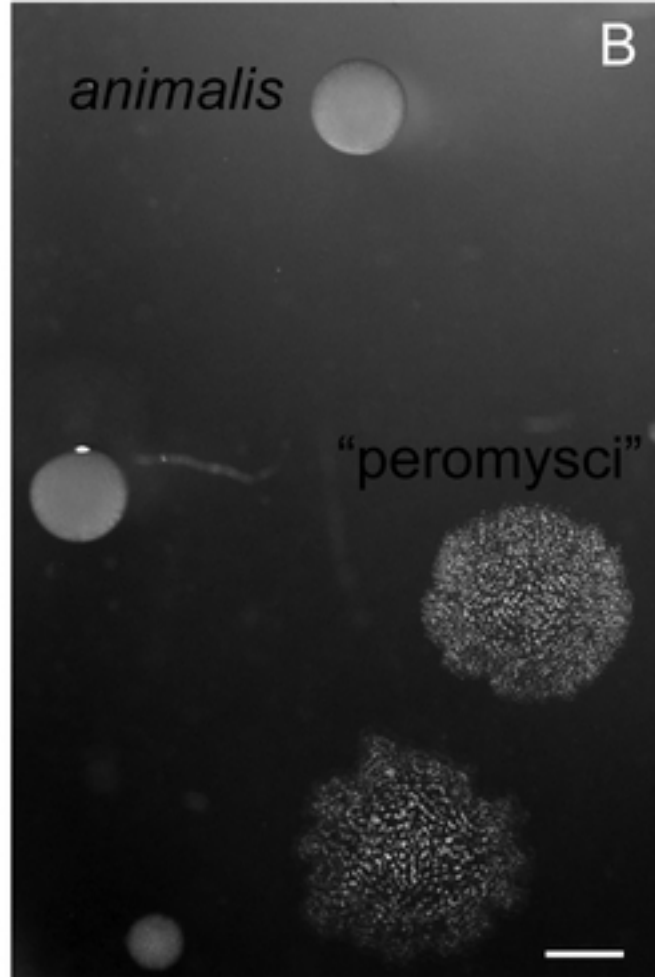
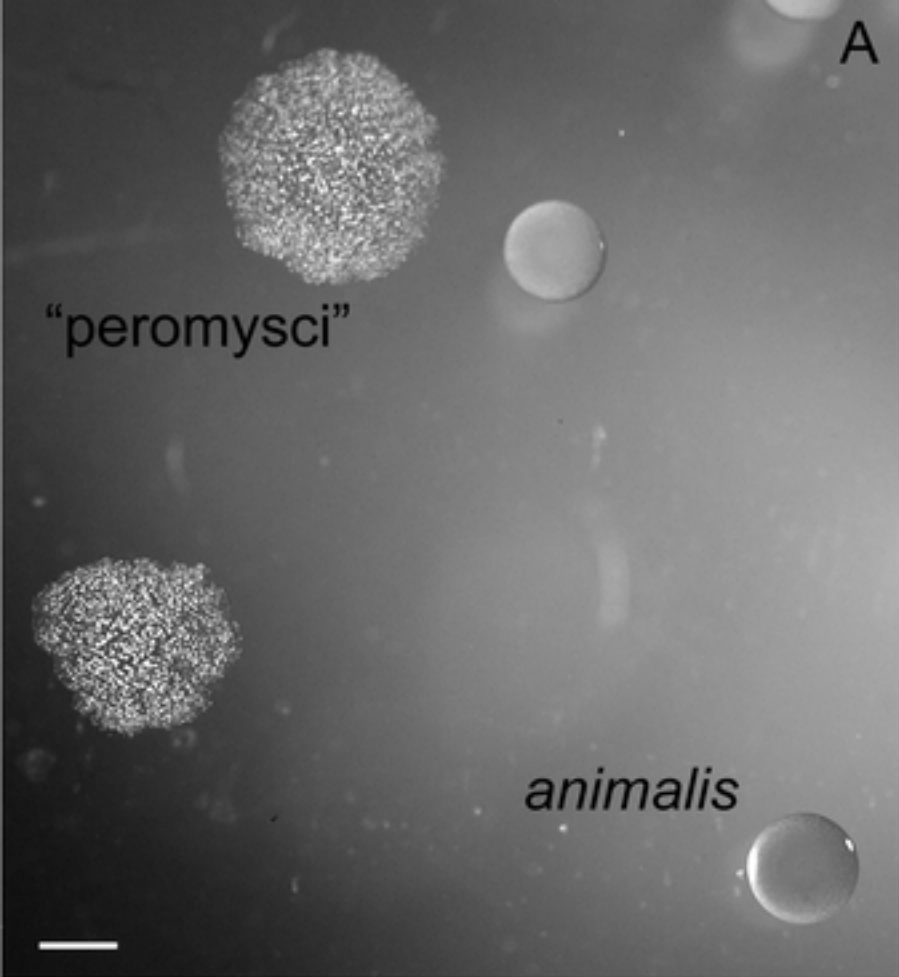


Figure 12

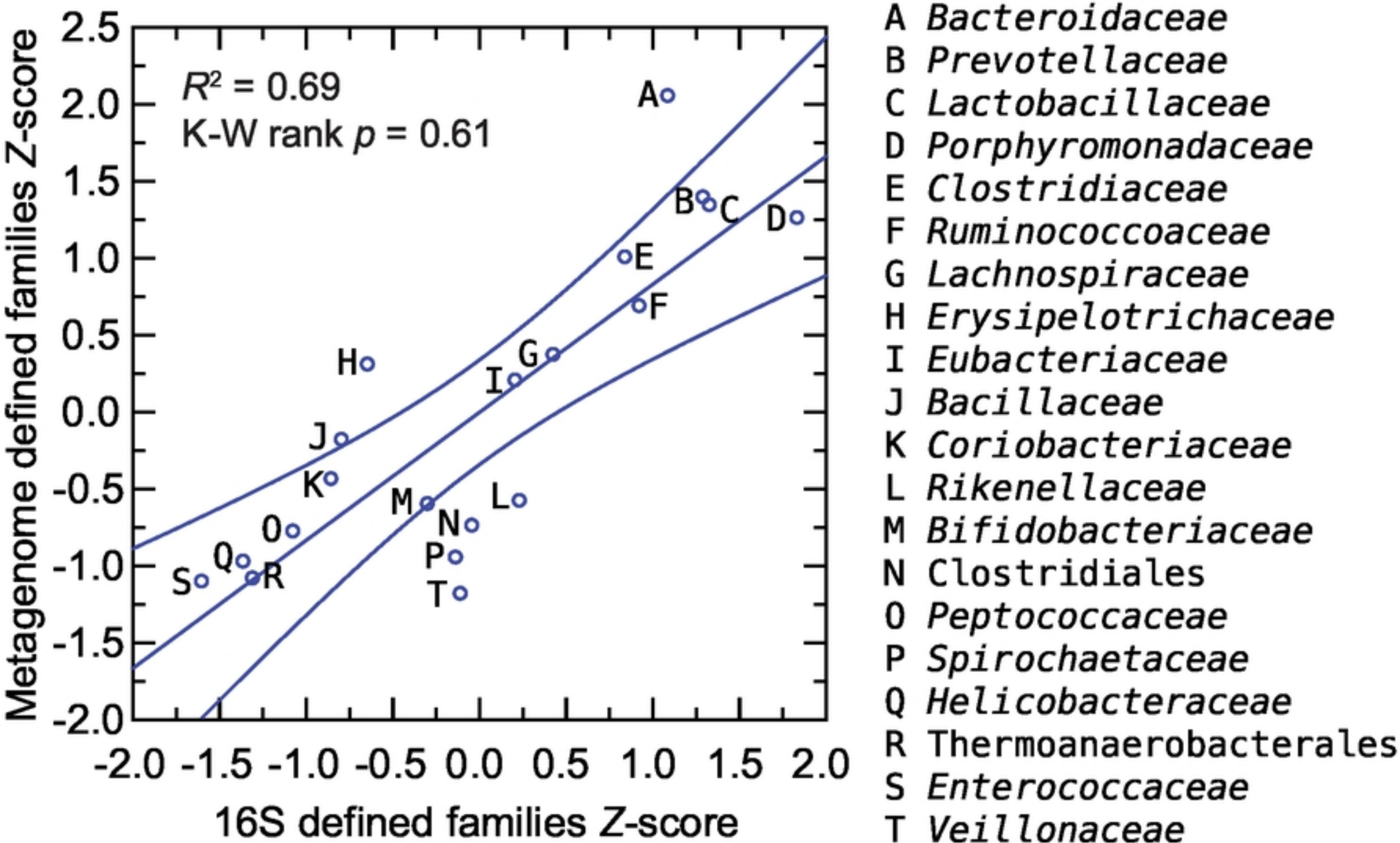


Figure 1

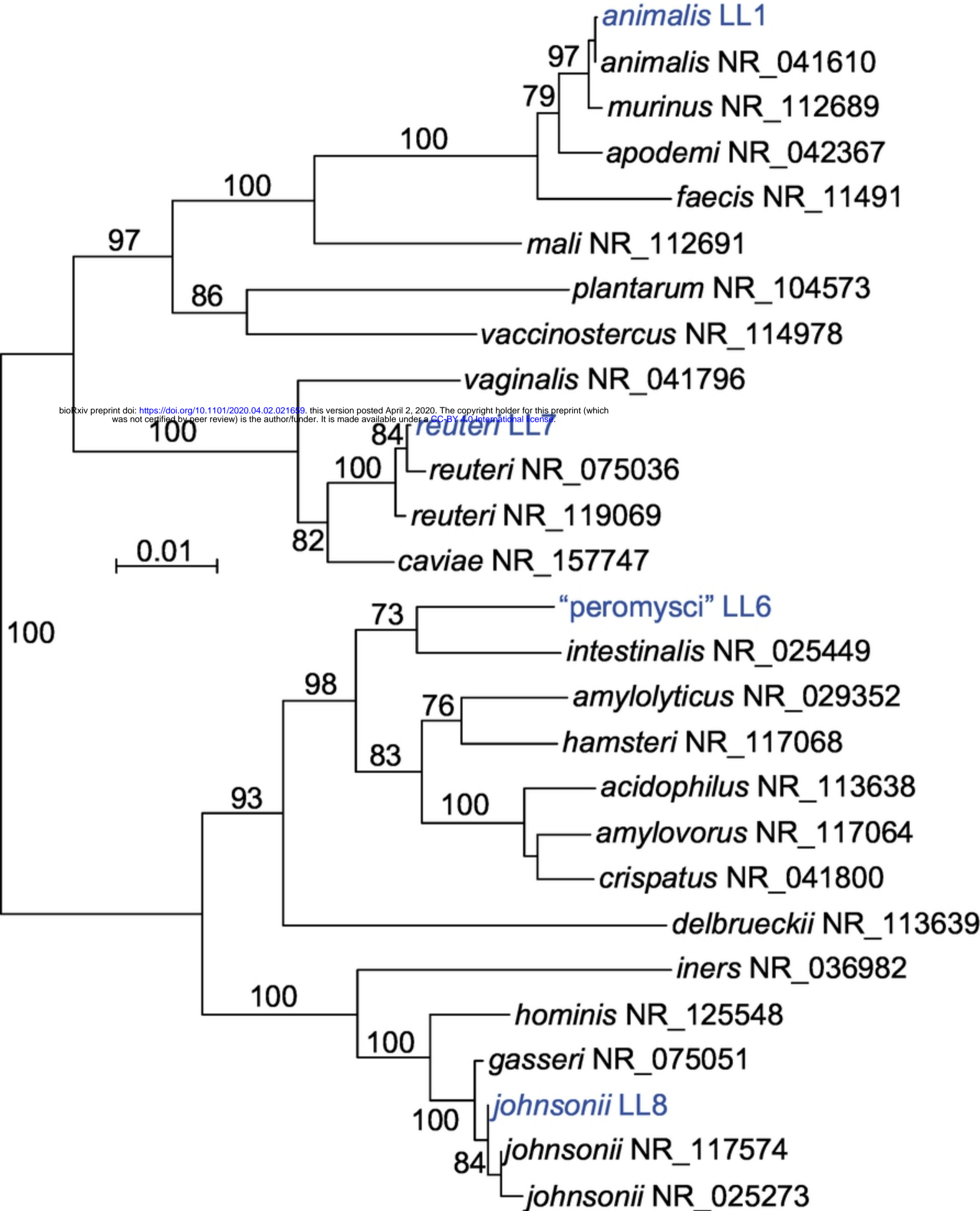


Figure 2



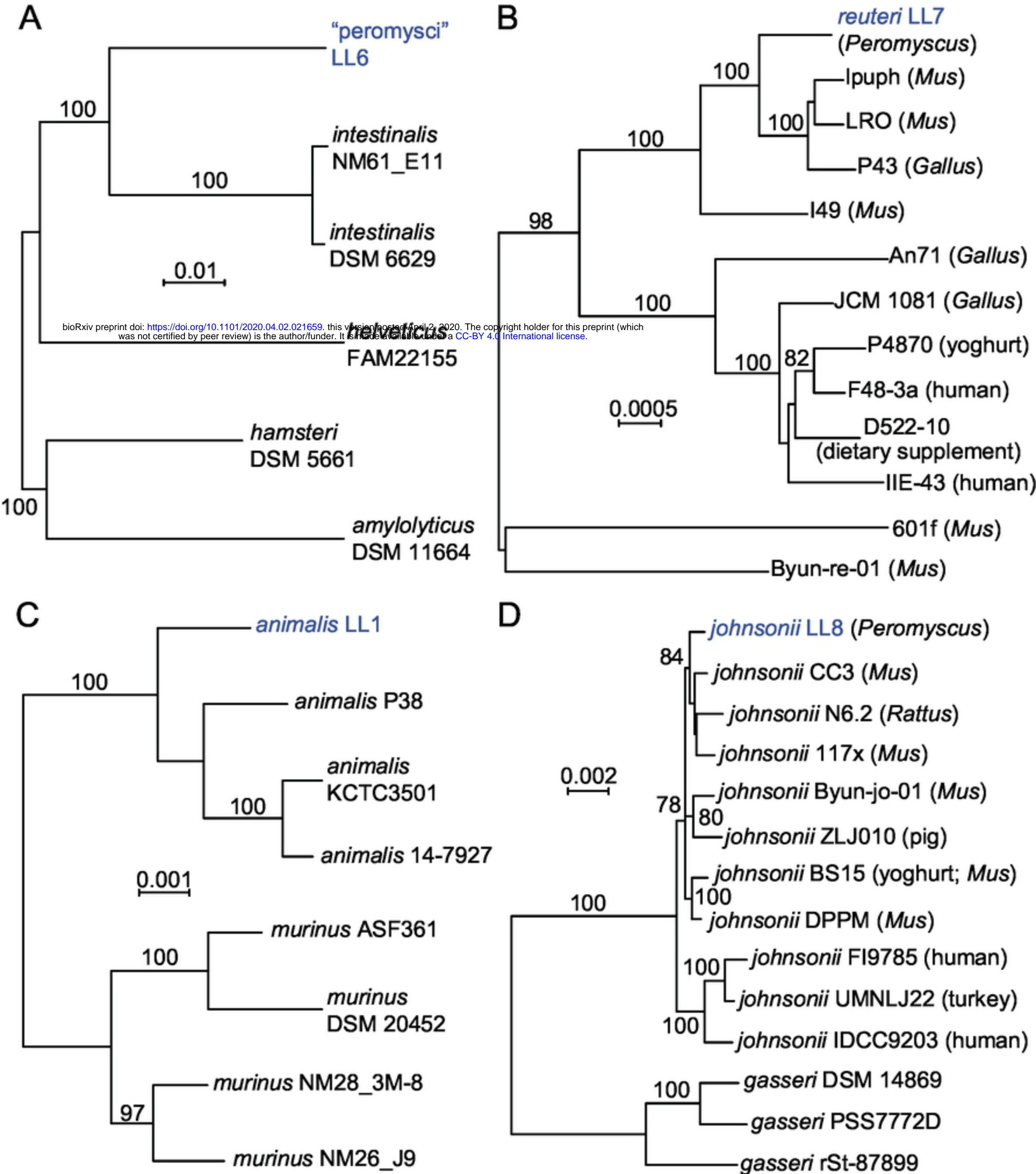


Figure 3





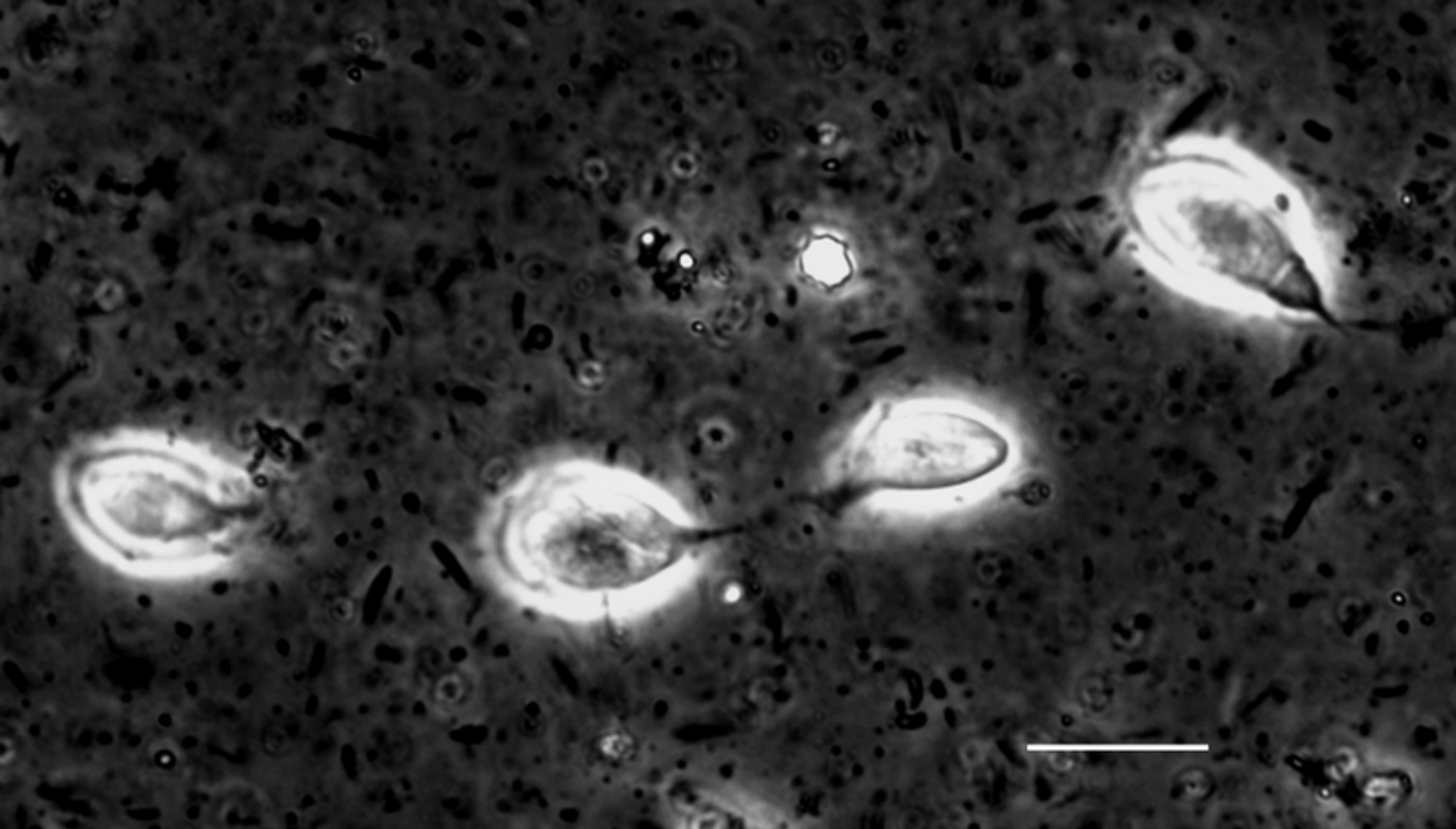


Figure 5

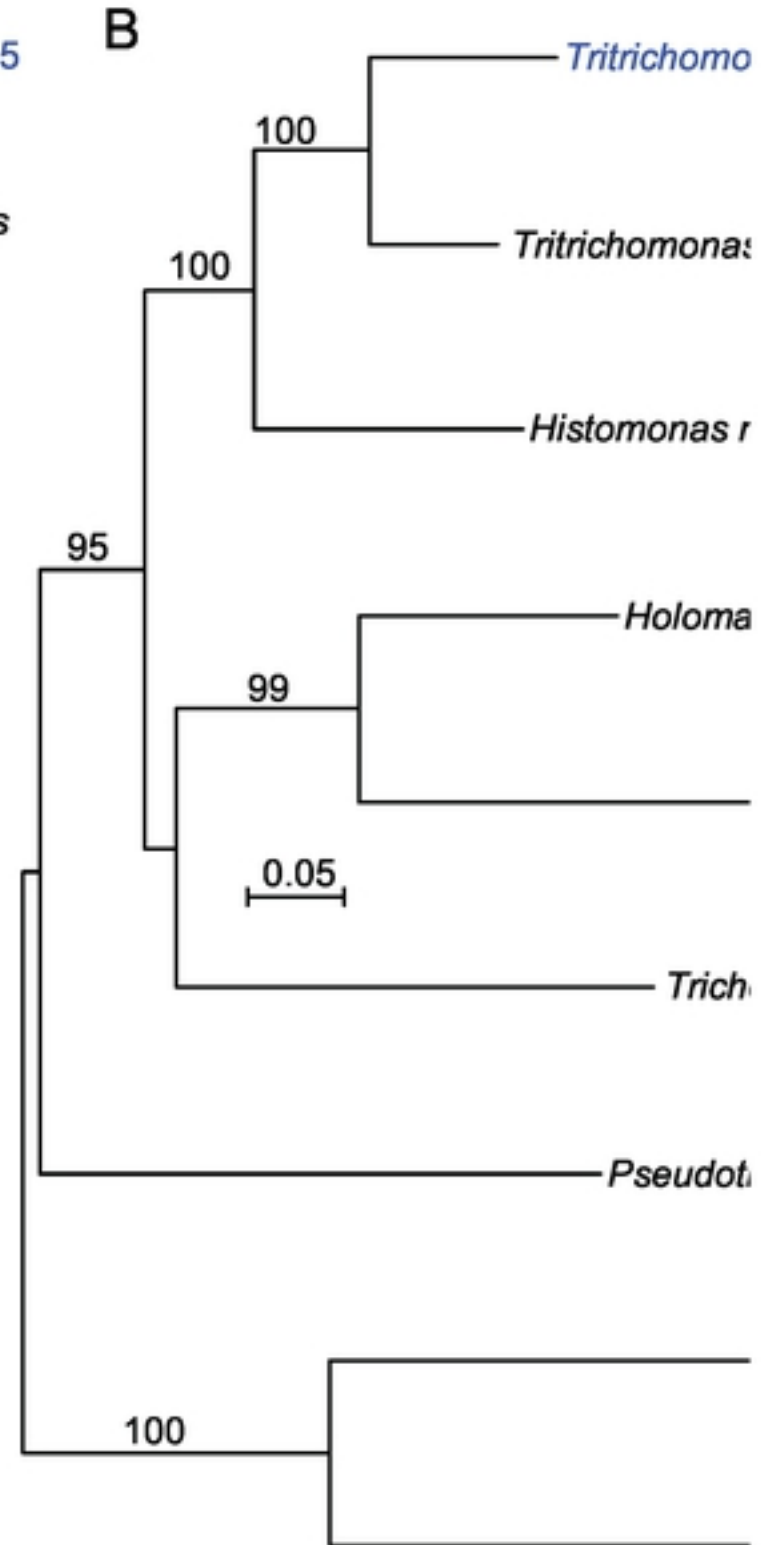
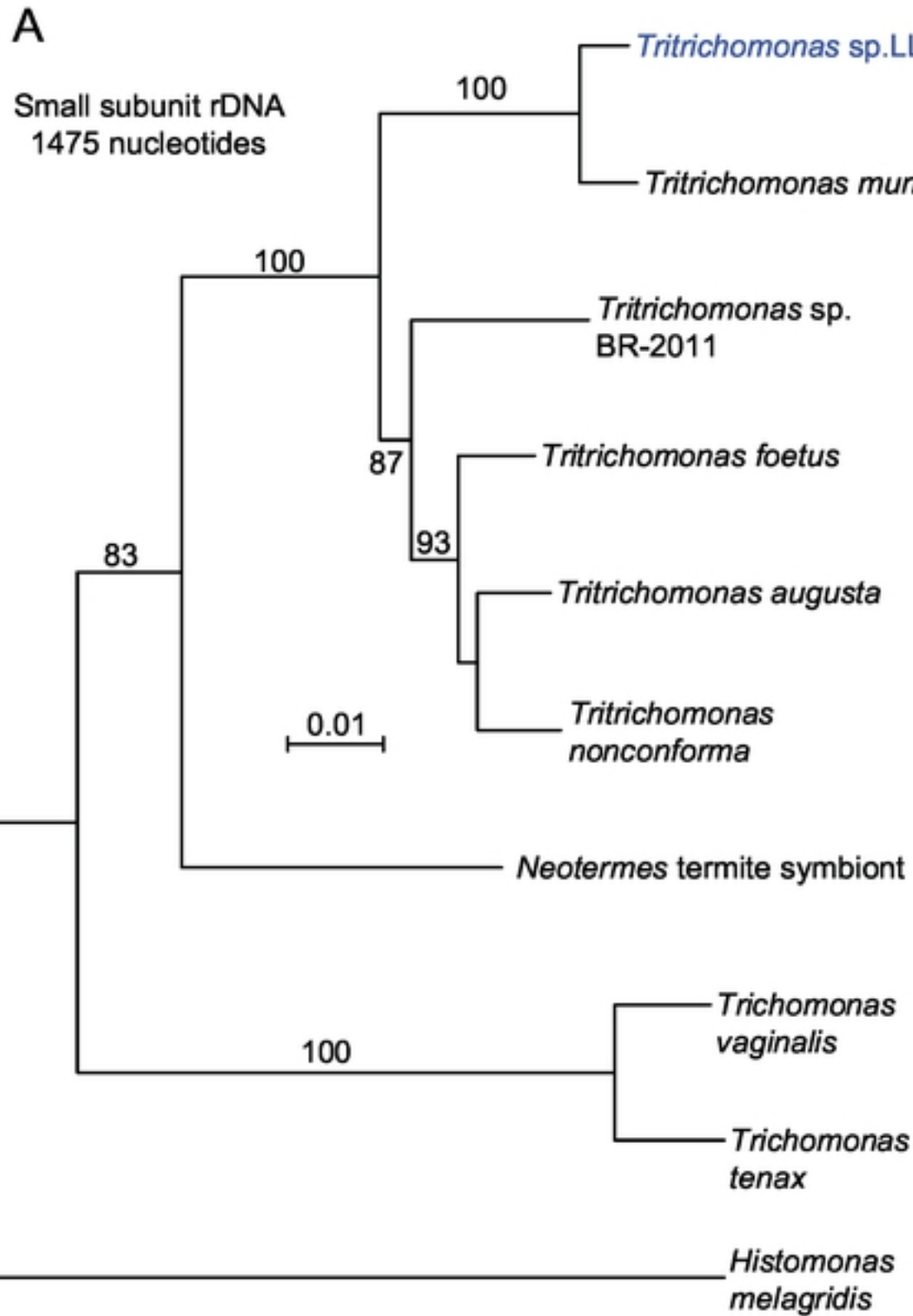


Figure 6

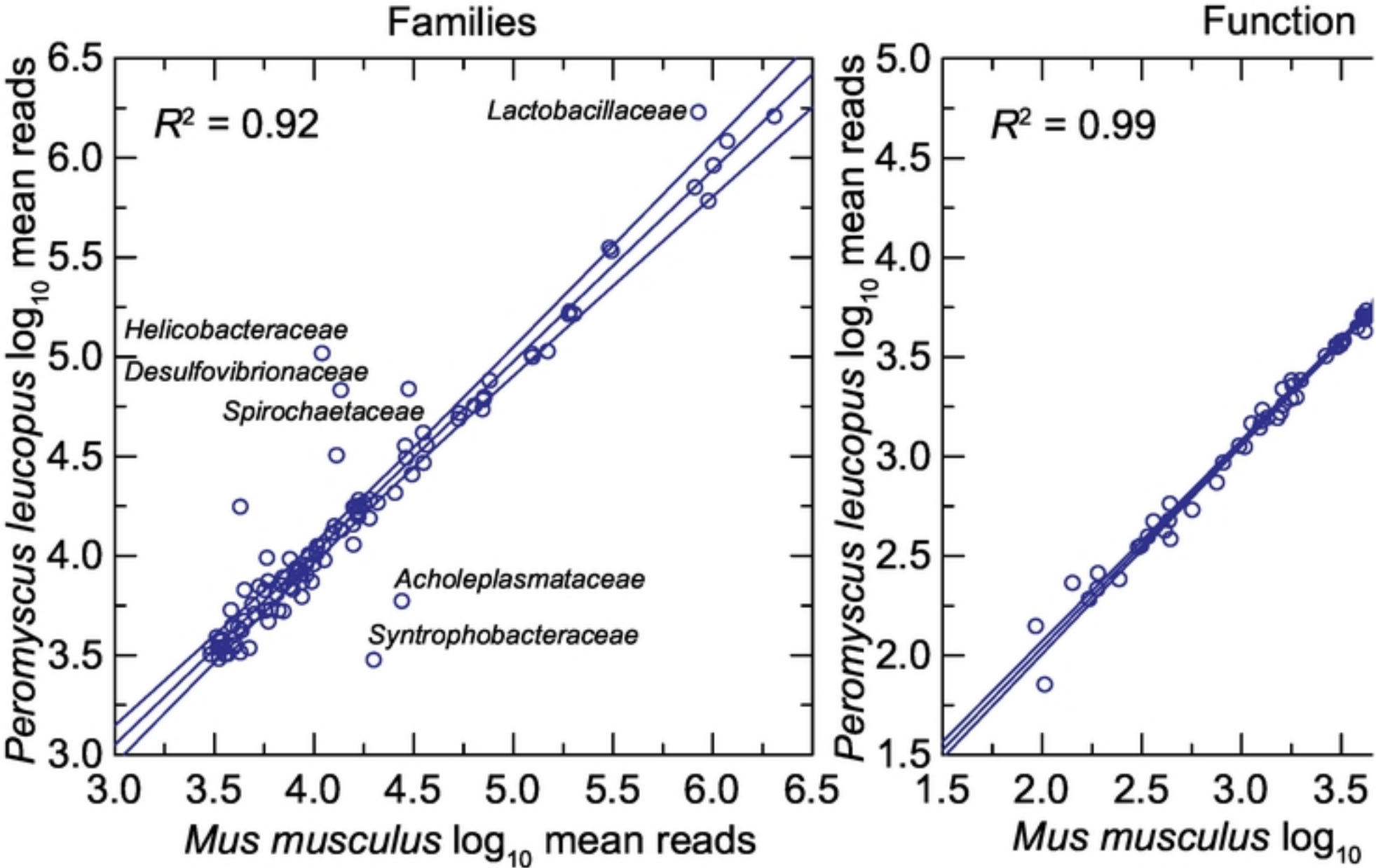


Figure 7



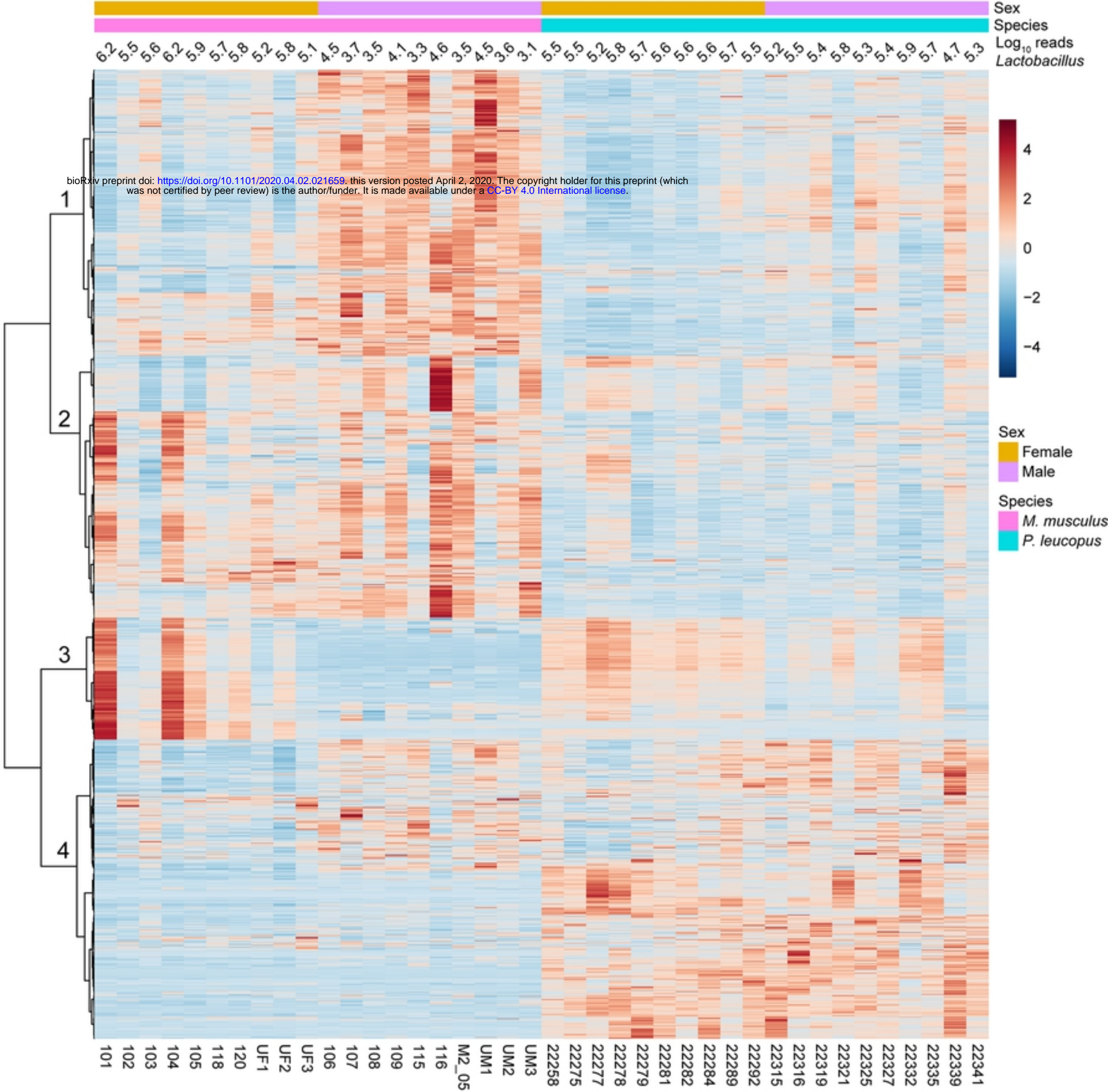


Figure 8

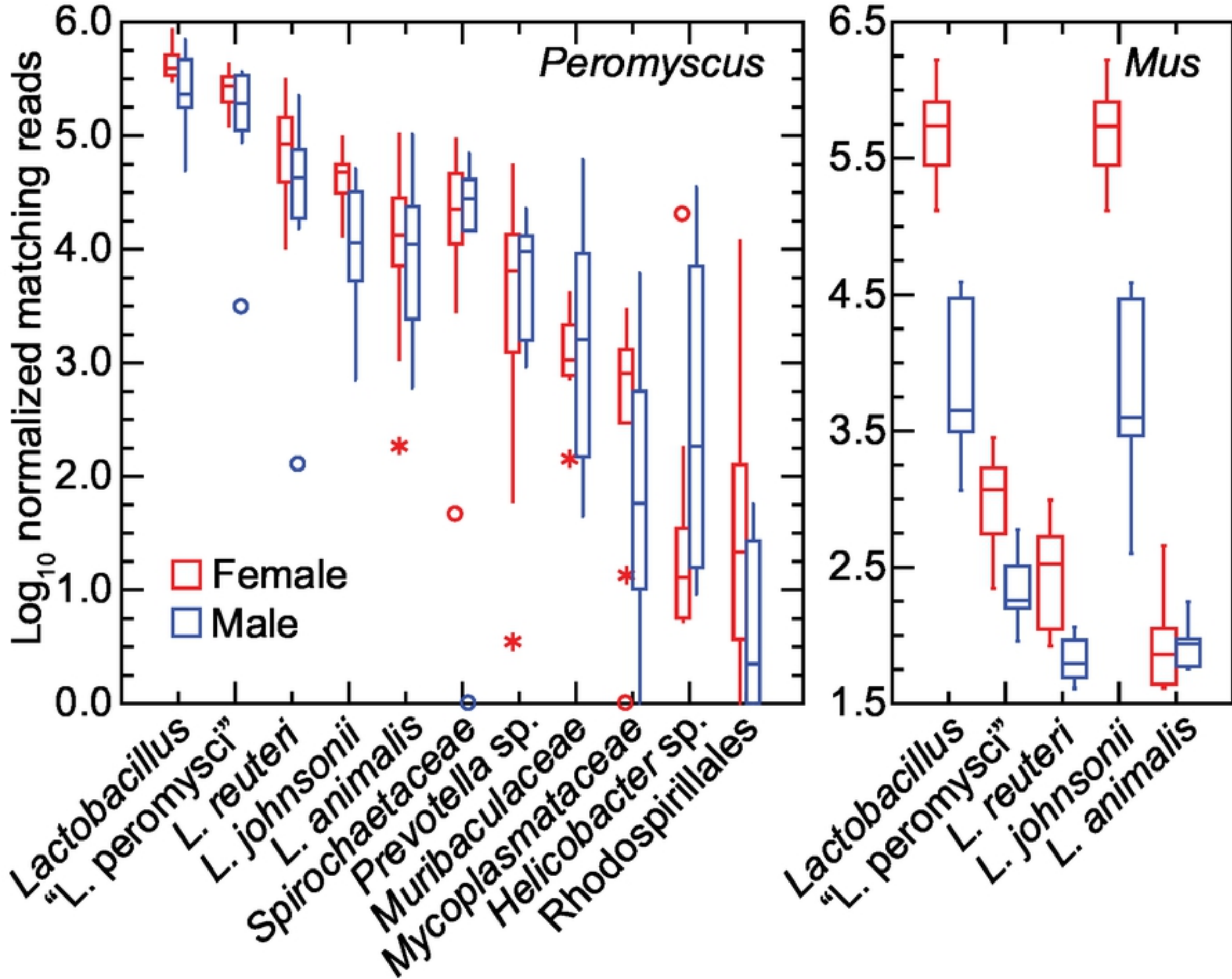


Figure 9

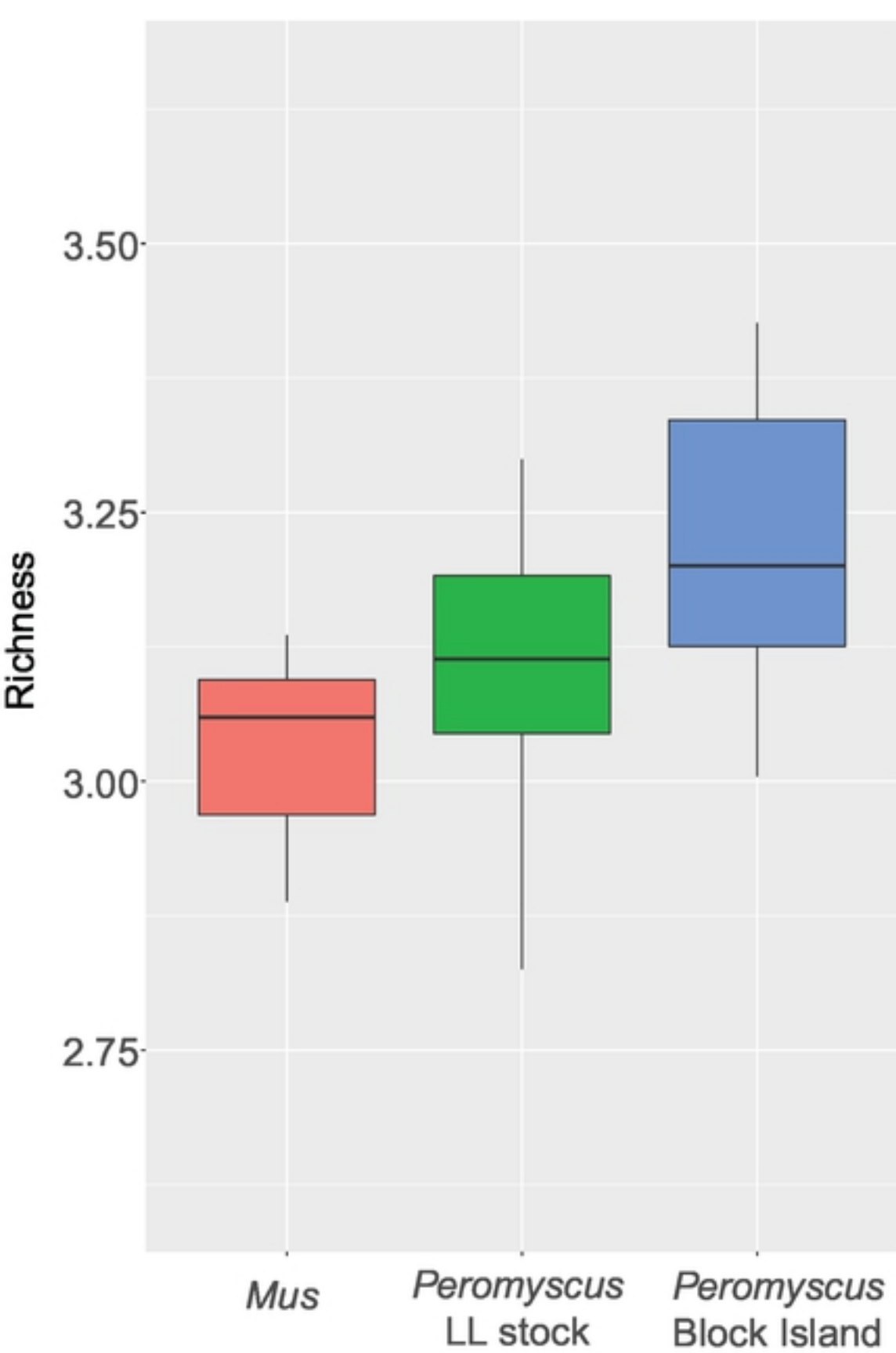


Figure 10



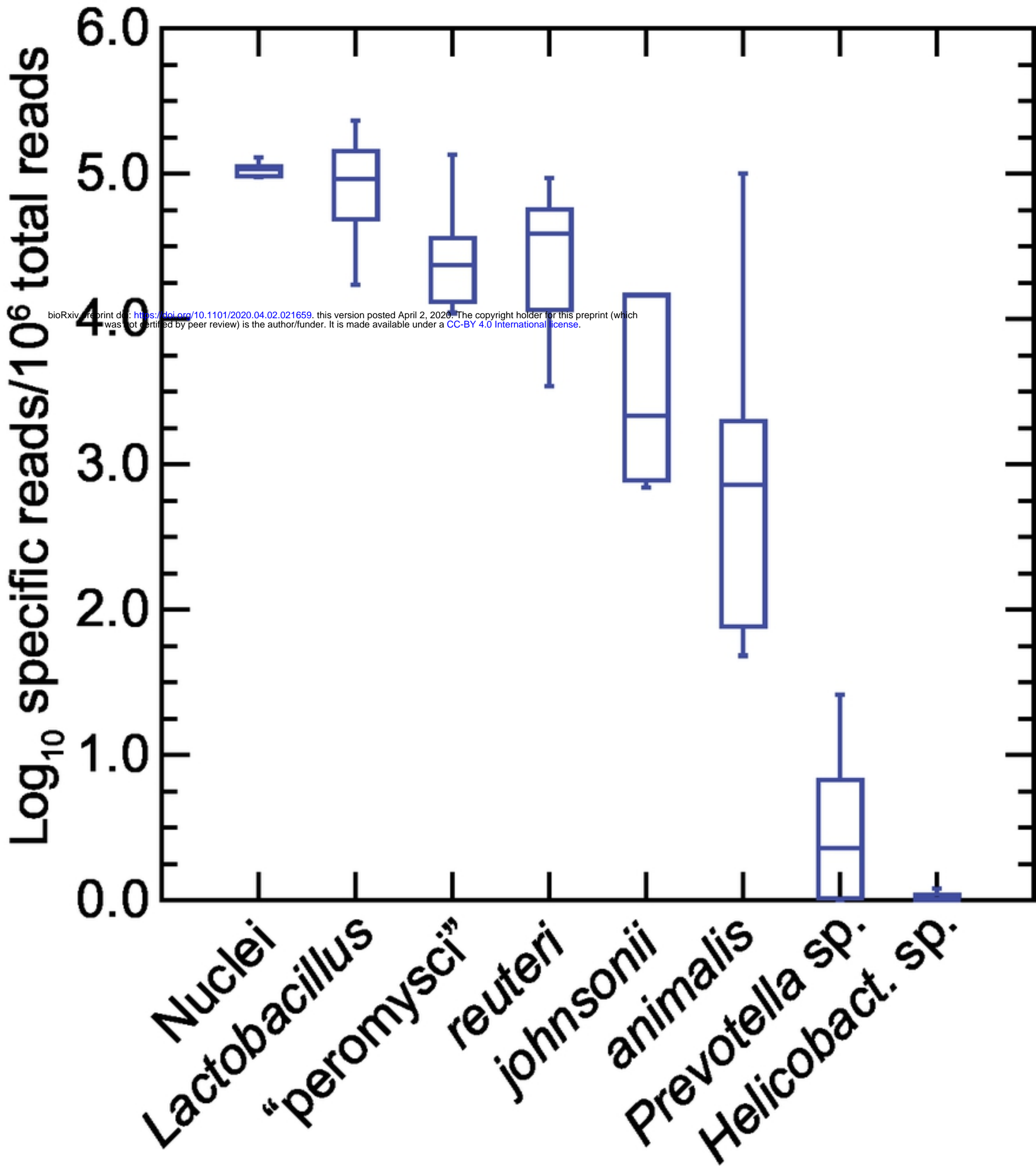


Figure 13

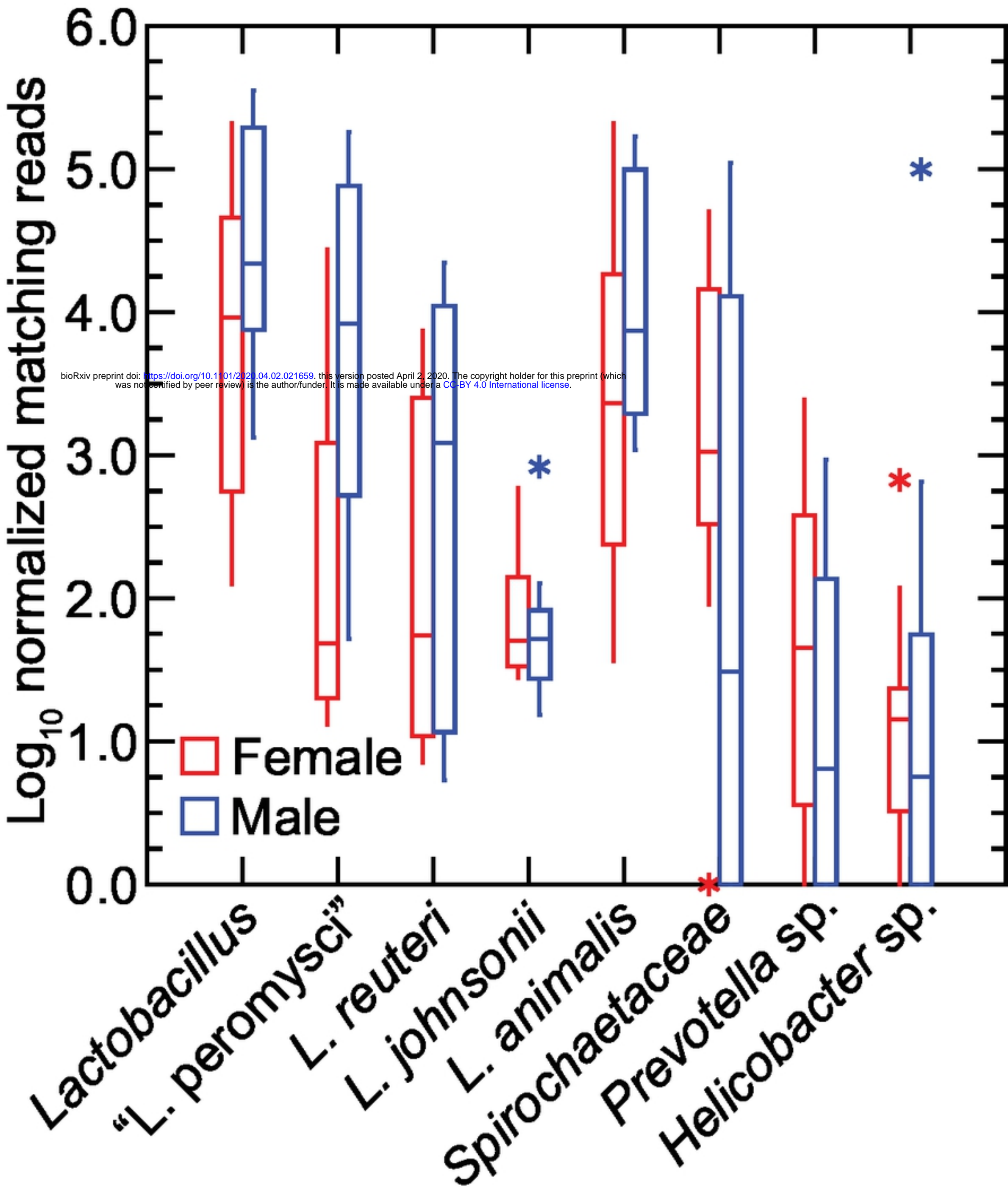


Figure 14



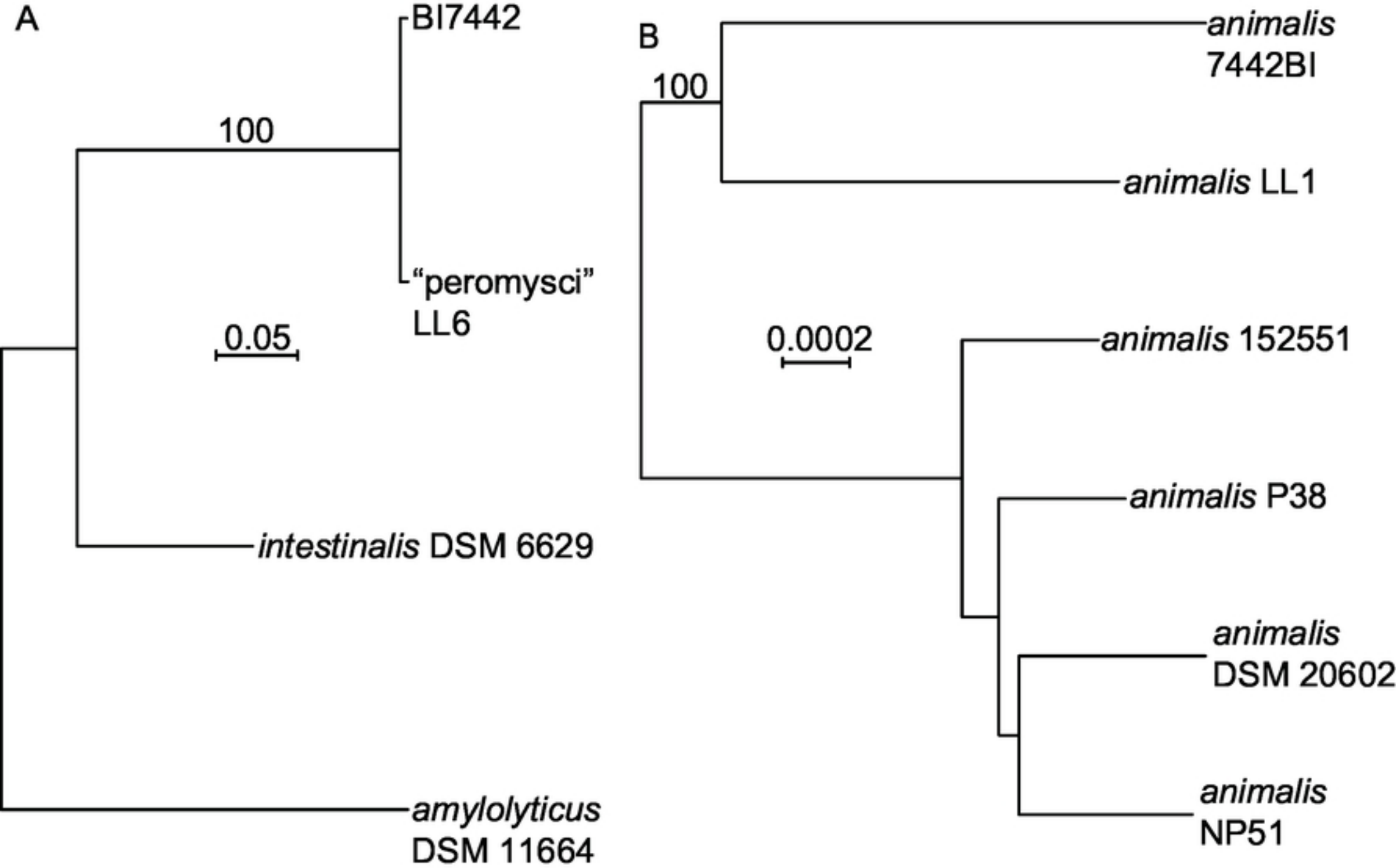


Figure 15